Piloted Simulation Evaluation of MTEs for the Assessment of Low-Level Handling Qualities

Tim Jusko
Research Engineer
German Aerospace Center (DLR)
Institute of Flight Systems
Braunschweig, NI, Germany

Tom Berger
Flight Controls Group Lead
U.S. Army Combat Capabilities Development
Command Aviation & Missile Center
Moffett Field, CA, USA

ABSTRACT

This study introduces three new proposed Mission Task Elements (MTEs) – "Big Air", "Giant Slalom", and "Super Combined" – aimed at evaluating handling qualities during low-level and high-speed flight profiles. These MTEs are designed to reflect operational task elements critical in military engagements, particularly where rotorcraft capabilities in evading radar detection and maneuvering at high speeds are paramount. Utilizing piloted simulations with four generic rotorcraft configurations under various flight control laws, the MTEs' effectiveness in exposing aircraft characteristics and handling deficiencies is systematically assessed. The evaluation, conducted with a diverse group of pilots, underscores the MTEs' relevance to real-world scenarios and their robustness in handling qualities assessment across different rotorcraft designs. The study reveals that while some configurations exhibit consistent Level 1 Handling Qualities Ratings (HQRs), others show varied performance, particularly when integrating additional means of velocity control, such as pusher propellers or velocity hold modes. Findings suggest modifications to current evaluation frameworks to better accommodate the dynamic operational requirements of future vertical lift platforms.

NOTATION

Symbols

$\Delta\eta$	Control displacement [%]
δ_c	Collective input [%]
δ_t	Thrust control input [%]
δ_x	Cyclic longitudinal input [%]
δ_y	Cyclic lateral input [%]
$\dot{\eta}$	Control displacement rate [%/s]
$\dot{\gamma}$	Flight path rate [deg/s]
$\dot{\psi}$	Yaw rate [deg/s]
$\dot{h}$	Vertical rate [ft/min]
γ	Flight path angle [deg]
ω	Natural frequency [rad/s]
ϕ	Roll attitude angle [deg]
ψ	Yaw attitude angle [deg]
τ	Phase delay [ms]
θ	Pitch attitude angle [deg]
A_η	Control attack metric [1/s]
D	Longitudinal parametric MTE gate spacing [ft]
DB_θ	Pitch attitude dropback [deg]
g	Acceleration due to gravity [m/s^2]
H	Vertical MTE gate spacing [ft]
h	Altitude [ft]
K	Gain [-]]
L	Lateral MTE gate spacing [ft]
n_z	Normal load factor [-]
p	Roll rate [deg/s]
q	Pitch rate [deg/s]
T	Time or time constant [s]
T_{θ_2}	Flight path-attitude lag [sec]
V	Airspeed [kn]
V_h	Maximum speed in level flight at maximum continuous power [kn]

Subscripts

adq	Adequate
BW	Bandwidth
des	Desired
nom	Nominal

INTRODUCTION

In the contemporary context of rotorcraft operations, the capability to perform at both low levels and high speeds is becoming increasingly vital for modern military engagements. This shift is underscored by the insights shared in a recent publication by the Joint Air Power Competence Centre (JAPCC), authored by Ichaso (Ref. 1), which draws lessons from recent conflicts to highlight the strategic advantages of rotorcraft capable of low-altitude flight for evading radar detection and high-speed maneuverability for extensive area coverage. These capabilities are essential for effective reconnaissance, assault, attack and surveillance in an era where advanced missile systems and unmanned aerial vehicles (UAVs) redefine the battlefield dynamics, necessitating rotorcraft that

Presented at the Vertical Flight Society's 80th Annual Forum & Technology Display, Montréal, Québec, Canada, May 7–9, 2024.

can swiftly adapt to these evolving threats and maintain air superiority.

In response to these emerging requirements, initiatives such as the NATO Next Generation Rotorcraft Capability (NGRC) program and the U.S. Future Vertical Lift (FVL) program are at the forefront of re-imagining military rotorcraft designs. These programs aim to transcend the limitations of traditional helicopters by exploring advanced configurations that promise superior performance metrics in speed, range, and efficiency. Innovations under consideration include lift-offset coaxial compound helicopters, tilt rotors, and single main rotor helicopters equipped with wings. These forward-thinking designs not only promise to redefine the operational capabilities of rotorcraft but also necessitate the development of new Handling Qualities (HQ) evaluation methods that reflect these advanced configurations and the novel mission profiles they enable, particularly at elevated speeds as discussed by Brewer et al. (Ref. 2) and Xin et al. (Ref. 3).

Need for Flight-Path-Focused MTEs

The U.S. military specification MIL-DTL-32742 (Ref. 4), building upon its predecessor ADS-33E-PRF (Ref. 5), is internationally acclaimed for setting the benchmark in both objective and subjective evaluation of handling qualities for rotorcraft. This specification serves as a foundational document in the U.S. and plays a significant role in the procurement and development projects within Germany and other countries. Despite its widespread acceptance and having been updated several times, the framework established by these standards reflects the technological and operational landscape of over three decades ago, focusing predominantly on traditional helicopter configurations and the operational paradigms prevalent at the time. Consequently, this has led to a gap in adequately addressing the needs of advanced rotorcraft configurations and certain mission profiles, especially high-speed forward flight and low-level maneuvering.

These mission profiles can be characterized as "flight-path focused" since the main objective that a pilot tries to achieve in the obstacle environment is to find and realize a flight path trajectory through the obstacle environment that minimizes exposure to enemy detection methods, meaning taking advantage of terrain covering at low levels.

Berger et al. (Ref. 6) explored the impact of response type selection and relevant handling qualities criteria and parameters, including Pitch attitude dropback (DB_θ), Control Anticipation Parameter (CAP), pitch bandwidth, and flight path bandwidth on Handling Qualities Ratings (HQR) within the context of attitude capture/hold and tracking tasks. One of the concluding remarks drawn from that study is that a flight path bandwidth requirement should be added to MIL-DTL-32742 (Ref. 4) to supplement the current flight path requirement. However, to do so, flight path-oriented tasks are needed to assess the location of the flight path bandwidth requirement level boundaries, as even designs with low values of flight path bandwidth received Level-1 ratings for pitch tracking tasks.

This study, conducted under the auspices of the US/German Project Agreement on Advanced Technologies for Rotorcraft (US/GER PA-ATR), seeks to address this need by proposing and evaluating flight-path-focused MTEs designed to assess the handling qualities of operational rotorcraft and emergent rotary-wing aircraft designs for low-level and high-speed mission profiles such as Nap-of-the-Earth (NOE) and contour flight (CF).

Previous Work

Pioneering research has significantly advanced the evaluation of rotorcraft low-level handling qualities. Notably, Pausder and Hummes (Ref. 7) study on BO 105 and UH-1D helicopters utilized statistical analysis to derive handling qualities metrics from pilot performance, demonstrating the importance of direct force control and reducing collective-to-pitch cross-coupling. The research of Landis and Aiken (Ref. 8) highlighted the advantages of small displacement controllers and the necessity for greater stability augmentation in Instrument Meteorological Conditions (IMC) for attack helicopters using piloted simulator experiments. Additionally, Bivens (Ref. 9) investigated directional handling for the LHX program [1], emphasizing the need for enhanced yaw damping to improve handling in low-altitude and air-to-air missions.

A limitation of these early studies was their reliance on non-rigorously defined flight tasks. Often, generic terrain paths were used, with pilots repeating the profiles to the best of their ability, such as in the Dolphin task. This approach lacked the precision of the MTE method in evaluating handling qualities.

Recent research efforts are actively bridging the gaps in rotorcraft HQ evaluations, particularly for high-speed flight scenarios that surpass the existing fleet's capabilities. These initiatives involve the introduction of novel MTEs tailored for high-speed assessments. Notable contributions include the exploration of Break Turns by Xin et al. (Ref. 3), Bumbaugh et al. (Ref. 10), and Berger and Ott (Ref. 11), alongside the investigation of high-speed acceleration/deceleration strategies by Brewer et al. (Ref. 2). Of note, these studies considered the available power margins of the configuration in question to calculate appropriate task performance requirements. This was done because, unlike in the hover/low-speed regime, high-speed flight and maneuvering are often limited by available power. The purpose of the MTEs is to evaluate HQ and not to drive performance requirements or penalize configurations with less available power. Therefore, MTE performance requirements were scaled to available power to create fair and configuration-agnostic HQ evaluations. This approach of scaling MTE performance requirements based on the available aircraft performance was the primary inspiration for the work presented in this paper. Additionally, significant advancements have been made in attitude capture and hold and attitude tracking, both documented by Klyde et al. (Ref. 12) and Klyde et al. (Ref. 13).

[1] The Light Helicopter Experimental (LHX) program was a 1980s United States Army helicopter procurement project to replace the AH-1 Cobra and OH-58 Kiowa helicopters, culminating in the RAH-66 Comanche prototype.

Overview

This paper proposes three new flight-path-focused Mission Task Elements (MTEs): "Big Air", "Giant Slalom", and "Super Combined". Following this, the Minimum Requirements Models (MRM) concept will be discussed to establish a foundation for deriving sensible MTE course sizes that accommodate changes in flight path due to pitch, roll, and collective inputs and take available aircraft performance into account. The discussion then extends to the description of the two simulation facilities, detailing the aircraft models employed and the flight control laws implemented for piloted simulation studies. In the results section, an analysis based on pilot feedback through questionnaires is presented. It evaluates the acceptance of the proposed MTEs alongside HQRs and task performance metrics for four distinct rotorcraft configurations. The paper concludes with a synthesis of findings. Recommendations are offered to enhance the precision and applicability of HQ evaluation methods for low-level and high-speed flight profiles.

PROPOSED TASKS

When discussing low-level flight, distinctions have to be made concerning the control method of vertical flight path change. Low-level flight maneuvers can be split into two main flight profiles: 1.) Nap-Of-the-Earth (NOE), where airspeed is sacrificed to get as close to the terrain as possible, maximizing coverage, and 2.) Contour flight (CF), where the airspeed is kept constant while the terrain contour is not matched as closely as in NOE. During NOE, the vertical flight path change is always achieved through pitch control; during CF, the control strategy highly depends on the rotorcraft configuration. For traditional helicopters, the maneuver has to be flown with collective controller inputs. Otherwise, the airspeed cannot be maintained. On the other hand, for compound helicopters with pushers or tilt-rotor aircraft, the vertical flight path can be changed using pitch control while maintaining speed. Both control strategies have to be addressed separately as variations of the proposed MTEs for a comprehensive maneuver set. Horizontal flight path change during low-level flight is achieved mainly through roll control for all considered configurations. Under these considerations, three new MTEs are proposed:

• **Big Air (BA) MTE** is a non-precise aggressive vertical flight path change task with the objective of checking for undesirable handling qualities during aggressive vertical flight path maneuvering. The suggested course layout is shown in Fig. 1. The detailed MTE description is given in Appendix A.

• **Giant Slalom (GS) MTE** is a non-precise aggressive lateral flight path change task aiming to check for undesirable handling qualities during aggressive lateral flight path maneuvering as well as evaluate turn coordination. The suggested course layout is shown in Fig. 2. The detailed MTE description is given in Appendix B.

• **Super Combined (SC) MTE** is a non-precise aggressive vertical and lateral flight path change task to check for undesirable handling qualities during aggressive vertical and lateral flight path maneuvering. Fig. 3 shows the suggested course layout. The detailed MTE description is given in Appendix C.

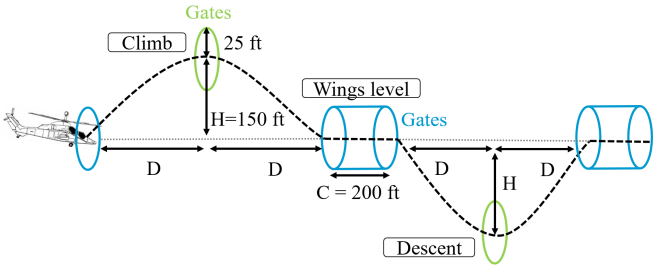

Figure 1. Suggested Big Air MTE course cueing.

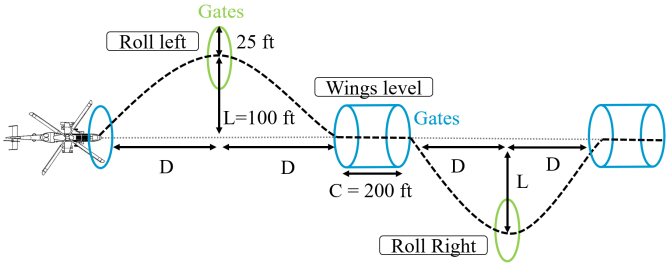

Figure 2. Suggested Giant Slalom MTE course cueing.

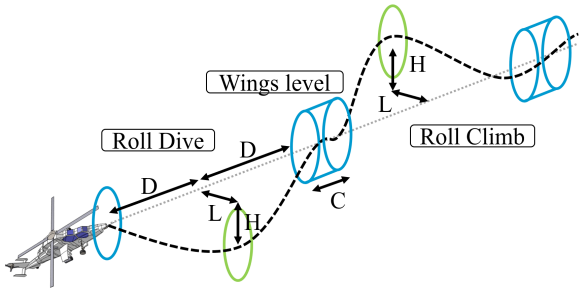

Figure 3. Suggested Super Combined MTE course cueing.

The general idea for these three MTEs is that the pilot has to fly through a series of gates that force lateral and/or vertical flight path changes (Fig. 1-3). To drive flight path precision demands during the task, the pilot has to fly through the gates within a 25 ft radius. Based on preliminary research and comprehensive discussions with pilots, these gates' lateral and vertical separation is set at $L = 100\,\text{ft}$ and $H = 150\,\text{ft}$, respectively. A "wings-level" segment of $C = 200\,\text{ft}$ is incorporated between sections requiring flight path changes. This segment aims to reset pilots to a neutral flight position following aggressive maneuvering. Note that Fig. 1-3 show only one half of each course, with the second being either a repetition or mirror-image of the first half.

Two sets of task performance criteria are established to address the CF and NOE flight profile aspects. For CF surrogate testing, the tasks restrict the allowable airspeed variation during maneuvers. For NOE surrogate tasks, maneuvers must be completed within the desired time limit T_{des}. This time limit is calculated using the longitudinal parametric course size D parameter, which will be discussed in detail in the following section.

Parametric course sizing 'D'

Maximizing the duration spent at low altitudes is essential to fully exploit the tactical benefits of low-level flight, thereby minimizing visibility and detection by adversaries. Consequently, pilots are encouraged to utilize the aircraft's full performance capabilities.

Therefore, the proposed tasks aim to explore potential HQ issues, such as cliffs or Pilot-Induced Oscillations (PIOs), that may arise from inceptor inputs during aggressive flight path adjustments near the aircraft's operational flight envelope (OFE). As a result, a fixed course sizing is impractical; instead, the course size, denoted as D is dynamically scaled based on the aircraft's airspeed, achievable rate of climb (ROC), and achievable normal load factor n_z. This approach enables pushing the task demand to the edge of the OFE, ensuring that potentially unachievable performance requirements are not imposed on the aircraft configuration. Furthermore, this flexibility permits the tailoring of MTEs to any point within the performance envelope, not just the OFE limit, catering to the specific needs of the operational flight profile. The course sizing D is calculated using a minimum requirement model simulation, which will be discussed in the next section.

This approach ensures the tasks assess the aircraft's handling qualities without imposing additional performance demands, distinguishing these tasks from traditional design by adopting and building on methods previously developed for the Break Turn and High-Speed Acceleration/Deceleration MTEs by Xin et al. (Ref. 3).

MINIMUM REQUIREMENTS MODEL

The following section describes the derivation and rationale of the Minimum Requirements Model (MRM), which is used to calculate the appropriate MTE course sizing parameter D values. The task performance requirements of the MTEs are constructed to be tailored to the primary input to change the flight path, namely cyclic pitch, cyclic roll, or collective. In the same vein, the models used are Single-Input-Single-Output (SISO), and the following section describes the three models used for each axis, respectively. For the following analysis, the airspeed V is assumed to be constant over the maneuver profile.

Cyclic Pitch - Flight Path Response Model

Pitch Rate Response In this analysis, the characteristics and implications of the Rate Command (RC) response type, the lowest level of augmentation defined (and allowed) in the detail specification MIL-DTL-32742 (Ref. 4) is examined. This response type is distinguished by its frequency response of K/s in the piloted crossover region, which manifests as a -20 dB/decade slope in the Bode plot across certain frequencies.

A crucial aspect of RC involves the pilot's interaction and control. Specifically, the pilot must close an attitude loop for stable flight, a particularly manageable task under good visual cueing conditions (UCE-1). However, in scenarios where visual cueing is degraded, or the pilot's attention is divided, the necessity for higher augmentation becomes evident. Closing an attitude loop is feasible with adequate visual cues, but flight tasks become considerably more challenging and workload-intensive when such cues are compromised. Therefore, MIL-DTL-32742 (Ref. 4) requires the use of RC in environments with effective visual cueing while prescribing more sophisticated augmentation systems for situations where visual cues are less reliable.

In rotorcraft HQ experiments reported by Key et al. (Ref. 14), pilots were found to favor rate-damped configurations, rating them highly (HQR 2-3) in fully attended NOE tasks with good visibility. Additions like Attitude Hold (AH) augmentation did not significantly alter these ratings or flying qualities. Thus, for aggressive NOE maneuvering in good visibility, the augmentation type, including attitude command/hold, was not crucial, leading to no specific response shape requirement in such conditions. RC response is also used to great success for desired command models used for model following control for high-speed configuration applications from hover up to speeds of 200 kn as shown by Berger (Ref. 15).

Only GVE conditions are considered during the presented MTE development, and an RC response type is assumed for the MRM's cyclic pitch response throughout the flight envelope. It should be noted, though, that due to the assumption of constant airspeed and the absence of external perturbations, the RC response type yields AH-like behavior when the simulated inputs are released into detent ($\delta_x = 0$).

The pitch rate response takes the form of a first-order transfer function:

$$\frac{q}{\delta_x}(s) = \frac{K_q e^{-\tau_\theta s}}{T_q s + 1} \tag{1}$$

Regarding HQ requirements, the MRM employed for the subsequent derivation of MTEs sizing parameter D is based on rate command. It is important to clarify that this does not necessitate the tested aircraft to be equipped with an RC system, and as shown later, the MTE was tested with other response types. However, the aircraft's response to control stick inputs must at least meet the performance standards established by this fundamental command type. This approach ensures that the evaluation of aircraft HQs is grounded in a consistent and quantifiable benchmark.

Given an estimate of the overall forward path time delay τ_θ, it is possible to tune the time constant of the first order rate

response model given in Eq. 2 to achieve a desired phase attitude bandwidth ω_{BW_θ} [based on the MIL-DTL-32742 (Ref. 4) definition of bandwidth, i.e., where the phase curve of the attitude response crosses -135 deg] for the attitude response given by:

$$\frac{\theta}{\delta_x}(s) = \frac{K_q e^{-\tau_\theta s}}{s(T_q s+1)} \tag{2}$$

$$1/T_q = \frac{-\omega_{BW_\theta}}{\tan(\tau_\theta \omega_{BW_\theta} - \pi/4)} \tag{3}$$

Next, the required pitch phase bandwidth ω_{BW_θ} is selected from the corresponding MIL-DTL-32742 (Ref. 4) requirement. Under the assumption of low values for the phase delay, a required bandwidth is selected from the Target Acquisition & Tracking Level 1 boundary with $\omega_{BW_\theta} = 2\,\mathrm{rad/s}$. The Level-1 requirement for maximum allowable time delay for the input to pitch attitude response is taken from the fixed-wing specification MIL-STD-1797 (Ref. 16) and is defined as $\tau_\theta = 0.1\,\mathrm{s}$. The time constant can now be obtained through Eq. 3 and yields $T_q = 0.33\,\mathrm{s}$.

Flight Path Response Aircraft operating on the frontside of the power-required curve are capable of flight-path control via control of pitch attitude as discussed by MIL-STD-1797 (Ref. 16). The short-term flight path response is related kinematically to the aircraft pitch attitude change by $1/T_{\Theta_2} \approx -Z_w$ and can be expressed as a first-order response model:

$$\frac{\gamma}{\theta}(s) = \frac{1}{T_{\theta_2} s+1} \tag{4}$$

MIL-STD-1797 (Ref. 16) further states that in general, $1/T_{\theta_2}$ is large enough to be of no concern for Conventional Take-Off and Landing (CTOL) aircraft in non-terminal flight phases of Category-A, which include "Terrain following" (TF). This, however, might not be the case for VTOL aircraft in general. Thus, a minimum value for the flight path bandwidth ω_{BW_γ} is selected based on the proposed boundaries by Berger et al. (Ref. 6). The minimum Level-1 bandwidth is selected as $\omega_{BW_\gamma} = 0.75\,\mathrm{rad\,s^{-1}}$. The respective time constant T_{θ_2} can again be obtained by the direct relationship between bandwidth and time constant for zero time delay ($\tau_\gamma = 0\,\mathrm{s}$):

$$T_{\theta_2} = 1/\omega_{BW_\gamma} = 0.75\,\mathrm{rad\,s^{-1}} \tag{5}$$

The maximum achievable pitch rate q_{max} at a steady state for full cyclic pitch control deflection $\delta_x = 1$ is limited by the maximum achievable normal load factor $n_{z,max}$ during pull-up:

$$K_q = q_{max} = \frac{g}{V}(n_{z,max} - 1) \tag{6}$$

Using Eq. 2, 4 and 6, the surrogate flight path angle response model due to cyclic pitch input becomes:

$$\frac{\gamma}{\delta_x}(s) = \frac{\theta}{\delta_x}\frac{\gamma}{\theta}(s) = \frac{\frac{g}{V}(n_{z,max}-1)}{s(0.33s+1)(s+1)} e^{-0.1s} \tag{7}$$

Control Strategy Assumptions The general assumption for the MRM simulations is that airspeed is kept constant and that the maximum achievable ROC ($\dot{h}_{max}$) is limited by the aircraft's available power. Furthermore, a step input control sequence is assumed, with the requirement that a step input shall not be shorter than 0.5 s. This is based on the idea that pilots will not move the cyclic stick from the trim-center position into full deflection and back to trim in less than that time.

Next, an optimization algorithm is used to determine the optimal step input sequence for the flight path response model to reach the set altitude of $H = 150\,\mathrm{ft}$ in the shortest time.

The optimal control strategy for pitch climb is assumed to be completed using step inputs only, as shown in Eq. 8:

1. The maneuver is initiated with a held full aft stick, developing pitch rate, attitude, and flight path rate until the maximum sustainable ROC is reached.
2. Next, the stick is released back to neutral at time T_1, which results in the pitch rate neutralizing again due to the RC response while maintaining attitude and ROC.
3. Shortly after T_1, the maximum positive normal load factor occurs coupled to the maximum flight path rate.
4. At the time T_2 full stick forward is commanded and held, developing a negative pitch rate and initiating the pitch down motion.
5. At time T_3, the stick is released again back to neutral.

$$\delta_x(t) = \begin{cases} +1 & 0 < t < T_1 \rightarrow \text{Pull-back} \\ 0 & T_1 < t < T_2 \rightarrow \text{Release} \\ -1 & T_2 < t < T_3 \rightarrow \text{Push-over} \\ 0 & T_3 < t \rightarrow \text{Neutralize} \end{cases} \tag{8}$$

Simulation Setup The states $q, \theta, \gamma, \dot{\gamma}$ as a function of time are directly obtained through the MRM simulations in the time domain. Furthermore, the normal load factor $n_z(t)$ can be expressed in terms of the flight path angles and rates obtained from the simulation data. An analytically simplified approximation to this relationship was derived by Thomson and Ferguson (Ref. 17) and will be used here for further analysis:

$$n_z(t) \approx \frac{V}{g}\dot{\gamma}(t, \delta_x(t)) + \cos(\gamma(t, \delta_x(t))) \tag{9}$$

Lastly, the ROC, expressed as $\dot{h}(t)$ can be calculated via the flight path angle:

$$\dot{h}(t) = V \sin\gamma(t, \delta_x(t)) \tag{10}$$

The completion time under this control strategy is then defined as the time needed to climb up to the targeted altitude of $H = 150\,\mathrm{ft}$ within $\pm 10\,\mathrm{ft}$. Therefore, for a climbing maneuver,

the ideal completion time T_{ideal} is achieved once the simulation reaches $h_{set} = 140\,\text{ft}$. The longitudinal distance during the maneuver is calculated under the assumption of constant airspeed.

With Eq. 8, 9 and 10, the optimization problem is defined and solved using the MATLAB *fminsearch* function, described by MathWorks (Ref. 18), under the optimization goals given in Eq. 11.

$$\text{Minimize:} \quad \min_{T_1,T_2,T_3} f(\delta_x(t)) = f_{n_z} + f_h + f_{\dot{h}} + f_\gamma + f_\theta + f_t \tag{11}$$

Where:

$$\begin{aligned}
f_{n_z} &= |n_{z,\text{set}} - \max(n_z(t))| && \rightarrow \text{set load factor} \\
f_h &= |h_{\text{set}} - \max(h(t))| && \rightarrow \text{set climb altitude} \\
f_{\dot{h}} &= |\dot{h}_{\text{set}} - \max(\dot{h}(t))| && \rightarrow \text{set ROC} \\
f_\gamma &= |\max(\gamma(t))| && \rightarrow \text{minimize flight path angle} \\
f_\theta &= |\max(\theta(t))| && \rightarrow \text{minimize pitch attitude} \\
f_t &= T_{\text{ideal}} && \rightarrow \text{minimize maneuver time}
\end{aligned}$$

Load Factor Considerations Fig. 4 presents an example of the simulation results for a velocity of $V = 100\,\text{kn}$ and $\dot{h}_{max} = 2000\,\text{ft}\,\text{min}^{-1}$ and varying values of $n_{z,set}$.

Four distinct cases arise from the comparison between the actual and nominal load factors, denoted as $n_{z,\text{OFE}}$ and $n_{z,\text{nom}}$, respectively. The aircraft's structural OFE limits and flight control constraints determine the actual load factor. In contrast, the nominal load factor is associated with the MTE geometry - specifically, it represents the minimum load factor required to achieve a specified ROC during a 150 ft climb. Figure 4 presents examples for the different cases by varying colors in the plot:

1. Case: **No n_z margin** ($n_{z,\text{OFE}} = n_{z,\text{nom}}$).
This represents a boundary case where the OFE performance precisely meets the nominal expectations. The pilot must adhere to a control strategy with no stick-to-detent period. After reaching the n_z steady state, the stick is held full aft until the maximum achievable ROC is achieved. Right afterward, the stick has to be pushed into the full forward position; if not, the climb will result in an overshoot of the 150 ft target altitude. This case is characterized by the observation that the steady state ROC will be reached only at a singular time along the trajectory.

2. Case: **Available n_z margin** ($n_{z,\text{OFE}} > n_{z,\text{nom}}$).
In this case, the system reaches the steady state of ROC earlier compared to case 1. This early attainment requires a moderated stick input to maintain the achieved value without surpassing the ROC limit. Consequently, this necessitates a "stick neutral phase" in the control strategy, enabling the completion of the MTE in a shorter duration than the nominal case. Importantly, the pilot does not need to exploit the full range of $n_{z,\text{OFE}}$ to achieve the desired task performance.

3. Case: **Non-usable n_z margin** ($n_{z,\text{OFE}} >> n_{z,\text{nom}}$)
Here, the available $n_{z,\text{OFE}}$ conflicts with the assumption that a step input cannot be shorter than 0.5 s. This results in an overshoot of the available ROC, leaving not enough power to maintain airspeed. This case also clarifies that a maximum load factor for a given ROC and V can be utilized for task performance improvement under the given assumption.

4. Case: **Inadequate n_z margin** ($n_{z,\text{OFE}} < n_{z,\text{nom}}$)
Conversely, this case highlights a situation where $n_{z,\text{OFE}}$ falls short of $n_{z,\text{nom}}$. Here, the desired ROC will only be reached beyond the midpoint of the ascent. Waiting to reach this point will result in exceeding the target altitude, necessitating a preemptive reversal in stick input to avoid overshooting, which would result in not achieving the desired ROC.

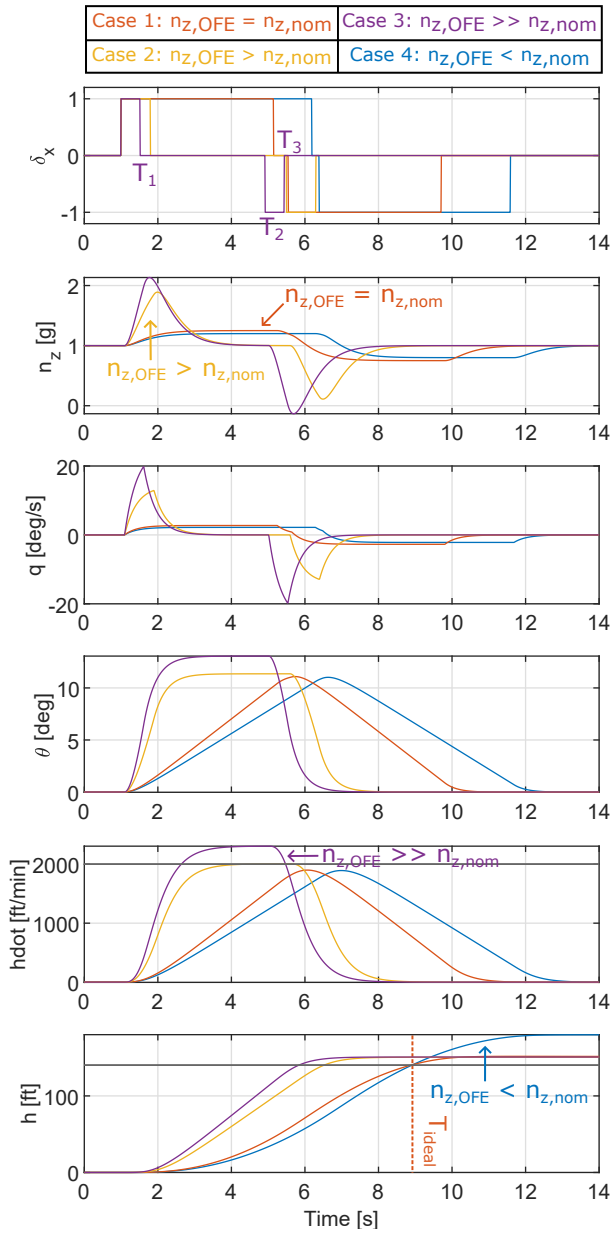

Figure 4. Example of MRM pitch-climb simulation for $V = 100\,\text{kn}$ (used for Big Air pitch-climb MTE sizing).

MTE Sizing Results To construct MTE sizing charts for the parametric distance D, first, the MRM simulation was run for varying nominal normal load factor $n_{z,\text{nom}}$ from 1.1 to 3.5, for constant airspeed ranging from 40 kn to 300 kn.

Fig. 5 shows the resulting contour plot for the course size D over varying airspeed and $n_{z,\text{nom}}$. As previously established, given a maximum achievable ROC constrained by available power, the nominal load factor $n_{z,\text{nom}}$ is required to at least briefly realize this ROC during a 150 ft climb maneuver. Therefore, each point on the contour plot can be matched to the maximum achieved ROC($n_{z,\text{nom}}$) during the simulated climb, which is shown in Fig. 6. This can be conceptualized as a starting point for MTE course sizing, representing the case where the scaling of D does not recognize available n_z overhead margins and, therefore, would not be part of the HQ evaluation envelope. This setup would potentially be insensitive to detecting HQ deficiencies that can occur if the configuration in question exceeds the nominal load factor, depending on whether or not the pilot chooses to use the available performance margins.

Exceeding $n_{z,\text{nom}}$ values leads to faster task completion, resulting in shorter ideal times (T_{ideal}) and required course sizing. This effect must be considered if the task ought to be tailored to an aircraft's available OFE performance envelope. Figures 7-10 illustrate the impact on D of varying values of $n_z \geq n_{z,\text{nom}}$ for constant values of ROC from 500 ft min^{-1} to 4500 ft min^{-1} and for the airspeed 60 kn, 100 kn, 160 kn and 220 kn. The resulting plots feature two distinct boundaries: The lower boundary, depicted as a dashed black line, represents the required $n_{z,\text{nom}}$ values for a specific velocity, below which the desired ROC is unattainable within the MTE geometry. A second boundary emerges (dashed red line) due to the minimum time assumption of 0.5 s for step inputs. Beyond this boundary, any surplus n_z, margin does not enhance task performance and may even detract from the aircraft's capability in terms of HQ evaluation by opening up the viable control strategy envelope of the pilots, thus also increasing the possibility for control strategy errors.

As ROC values increase, these boundaries start to converge, merging at values greater than 3000 ft min^{-1}, where variations in D due to changes in n_z become small and, for MTE testing, negligible. The influence of n_z on D for a given ROC and velocity V is more pronounced at lower ROC values, significantly affecting course sizing below 3000 ft min^{-1}. This analysis introduces the concept of scalable MTE design, highlighting performance and structural requirements delineated by the two n_z boundaries. Values below the left boundary indicate unutilized ROC/power margins for NOE/CF tasks, while values beyond the right boundary imply excess n_z margins that do not contribute to task performance.

It should be noted that surprisingly, by starting with an arbitrary selection of ROC suitable for the aircraft's performance envelope leads to design guidelines on minimum and maximum load factor values for the MTEs in question. This approach parallels the performance requirements outlined in MIL-DTL-32742 (Ref. 4) for static task performance requirements, but unlike fixed values, the scalable MRM method produces performance boundary curves.

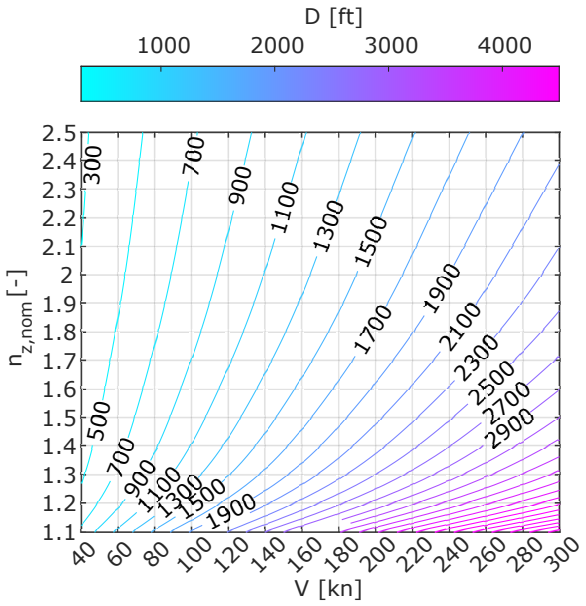

Figure 5. Big Air pitch climb MTE course size D vs. velocity V and nominal load factor $n_{z,\text{nom}}$

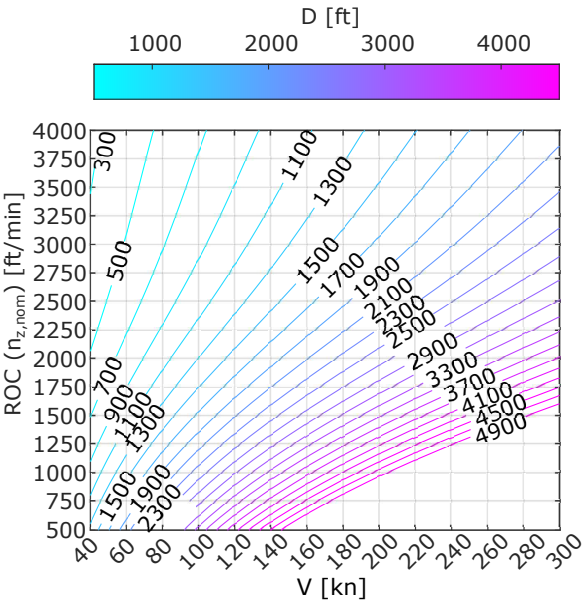

Figure 6. Big Air pitch climb MTE course size D vs. velocity V and ROC (for nominal load factor $n_{z,\text{nom}}$ values)

Collective - Flight Path Response Model

Heave Rate Response The response to collective in forward flight is considerably more complicated than in hover. While collective pitch remains the principal control for vertical velocity and flight path angle up to moderate forward speed, pilots normally use a combination of collective and cyclic

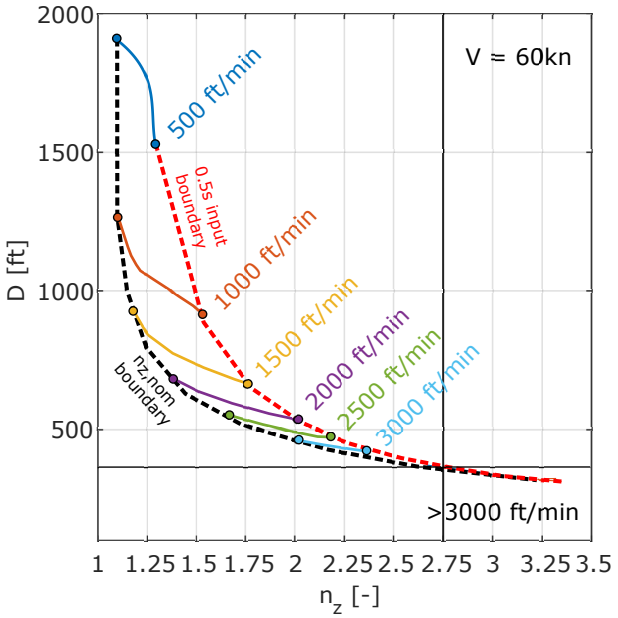

Figure 7. Big Air pitch climb MTE sizing chart: D values vs. n_z and $\dot{h}$ at $V = 60$ kn

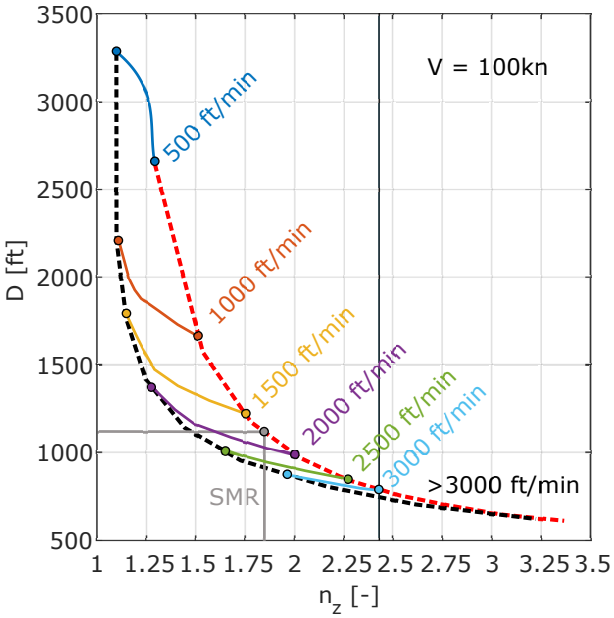

Figure 9. Big Air pitch climb MTE sizing chart: D values vs. n_z and $\dot{h}$ at $V = 100$ kn

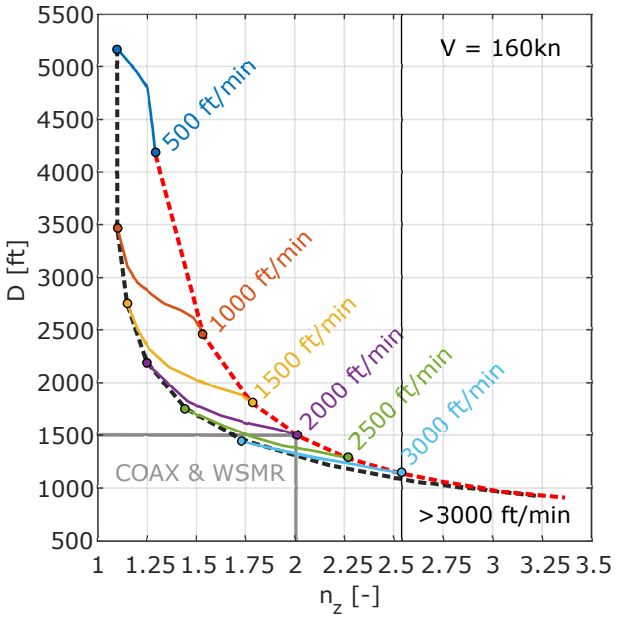

Figure 8. Big Air pitch climb MTE sizing chart: D values vs. n_z and $\dot{h}$ at $V = 160$ kn

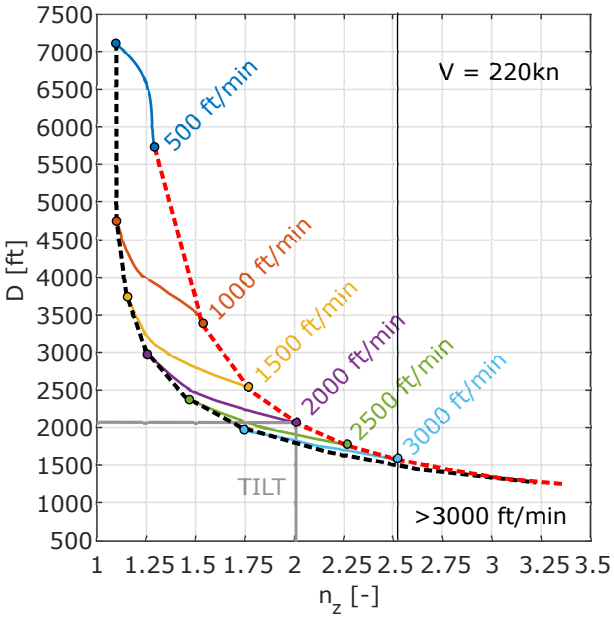

Figure 10. Big Air pitch climb MTE sizing chart: D values vs. n_z and $\dot{h}$ at $V = 220$ kn

to achieve transient flight path changes in high-speed flight. Also, collective pitch inputs are typically coupled to powerful pitch, roll, and yaw moments in forward flight, as discussed by Padfield G. D. (Ref. 19).

The current requirements on vertical axis response characteristics in MIL-DTL-32742 (Ref. 4) are based on the premise that the height rate response should have a qualitative first-order shape for at least 5 s following collective (δ_c) step input, as described by Eq. 12.

$$\frac{\dot{h}}{\delta_c}(s) = \frac{K_{\dot{h}} e^{-\tau_{\dot{h}} s}}{T_{\dot{h}} s + 1} \tag{12}$$

Ockier (Ref. 20) showed that during flight test evaluation of this requirement using the Bo-105, the pitch response to a collective step is very strong, causing the speed to reduce and the aircraft flight path to change as the nose pitches up. A first-order height rate response was achievable though when applying additional cyclic pitch to minimize pitch attitude ex-

cursions. Based on this; the premise that the vertical response should adhere at least to a first-order model under corrective pitch inputs to minimize airspeed excursions is adopted for further modeling. The required time constants in MIL-DTL-32742 (Ref. 4) for Level 1 are given by $T_{\dot{h},L1} \leq 5\,\mathrm{s}$ and $T_{\dot{h},L2} \leq 10\,\mathrm{s}$ for Level 2.

In the opinion of the authors, these values do not reflect the intention to drive requirements for future vertical lift configurations: Ockier (Ref. 20) further showed that for systems with a time constant close to or larger than the 5 s limit, estimation of the time constant becomes very difficult. For such systems, the vertical rate does not reach a steady state within the observation window, and the gain $K_{\dot{h}}$ in Eq. 12 cannot be accurately estimated. Without a valid $K_{\dot{h}}$, estimations of the time constant $T_{\dot{h}}$ are arbitrary.

Padfield (Ref. 21) discussed that most present-day helicopters should have no difficulty meeting the Level 1 requirement on $T_{\dot{h}}$. The values of Z_w for conventional helicopters support this: in the presence of a reasonable good rotor RPM governing, negligible system lags or time delays, $1/T_{\dot{h}}$ is well approximated as $-Z_w$. Furthermore, discussions with experienced pilots suggested that the previously considered time constants were excessively lenient for aircraft designed for low-level, high-speed maneuvering. For instance, with a time constant of 5 s, it would require approximately 10 seconds to attain 86.5% of the steady-state vertical rate, which could be suboptimal in demanding flight scenarios.

To ensure that the MRM aligns more closely with values that the authors believe are representative of the performance standards expected of advanced future vertical lift configurations, the time constant values are adjusted to $T_{\dot{h},L1} \leq 2.5\,\mathrm{s}$ and to $T_{\dot{h},L2} \leq 5\,\mathrm{s}$. This adjustment aims to provide a more rigorous benchmark for evaluating aircraft performance, particularly in scenarios requiring swift and precise maneuverability in NOE environments.

Control Strategy Assumptions As previously discussed, an optimization algorithm is used to determine the optimal step input sequence for the heave rate response model to reach a set altitude of $H = 150\,\mathrm{ft}$ in the shortest amount of time. The optimal control strategy for collective climb is assumed to be completed using step inputs only:

1. The maneuver is initiated with full collective up, developing heave rate and a positive ROC as quickly as possible.
2. At time T_1, the collective is commanded and held full down, neutralizing the positive ROC in the shortest time possible.
3. At the time T_2, the collective is released again back to neutral after reaching the desired altitude.

$$\delta_c(t) = \begin{cases} +1 & 0 < t < T_1 \rightarrow \text{Raise collective} \\ -1 & T_1 < t < T_2 \rightarrow \text{Lower collective} \\ 0 & T_2 < t \rightarrow \text{Neutralize} \end{cases} \tag{13}$$

The states $\dot{h}$ and h as a function of time are directly obtained through the MRM simulations in the time domain. The ideal completion time T_{ideal} under this control strategy is then defined as the time needed to climb up to the targeted altitude of $h_t = 150\,\mathrm{ft}$ within $\pm 10\,\mathrm{ft}$. The ideal completion time is achieved once the simulation reaches $h_{set} = 140\,\mathrm{ft}$. The longitudinal distance covered during the maneuver is calculated under the assumption of constant airspeed.

With Eq. 12 and 13 the optimization problem is defined and solved using the MATLAB *fminsearch* function. The optimization functions are given by Eq. 14 and Fig. 11 shows an example of the simulation results for $V = 60\,\mathrm{kn}$.

As the heave rate gain $K_{\dot{h}}$ increases, diminishing returns in achieved ROCs start to show. This behavior arises due to the introduction of a task geometry, where high ROC values cannot be realized during a 150 ft climb without overshooting the altitude target. For the 60 kn case, $K_{\dot{h}} > 2000\,\mathrm{ft\,s^{-1}}$ show significant decrease in achievable ROC. This, in turn, impacts the rate of decrease in task completion time and course sizing.

$$\text{Minimize:} \quad \min_{T_1,T_2} f(\delta_c(t)) = f_h + f_{\dot{h}} + f_t \tag{14}$$

Where:

$$\begin{aligned} f_h &= |h_{\text{set}} - \max(h(t))| && \rightarrow \text{set climb altitude} \\ f_{\dot{h}} &= |\dot{h}_{\text{set}} - \max(\dot{h}(t))| && \rightarrow \text{set ROC} \\ f_t &= T_{\text{ideal}} && \rightarrow \text{minimize maneuver time} \end{aligned}$$

MTE Sizing Results To construct MTE sizing charts for the parametric distance D, first, the collective climb MRM simulation was run for varying ROC from $500\,\mathrm{ft\,min^{-1}}$ to $3500\,\mathrm{ft\,min^{-1}}$, for constant airspeed ranging from 40 kn to 140 kn.

Fig. 12 displays the resulting contour plot, illustrating the course size D as it varies with airspeed and ROC. This visualization reveals points of diminishing returns in course sizing, represented by a line (dashed black line) across the velocity spectrum, where the rate of change in D decreases with increasing ROC values.

Notably, at approximately $3400\,\mathrm{ft\,min^{-1}}$, the reduction in D relative to the increase in ROC becomes negligible. This observation establishes an upper limit boundary for useful ROC within the context of MTE evaluation for the specified task geometry (dashed red line).

Reaction Time Modification

During initial testing, it became clear that the incorporation of additional reaction time into the MRM was needed. Especially for course sizing, in which the collective axis is the primary flight path change input, the pilots found that they demanded excessive control compensation to reflect operational pilot control strategies. This is grounded in the assumption of step inputs for course size calculation, which a pilot cannot replicate during piloted simulations or flight testing.

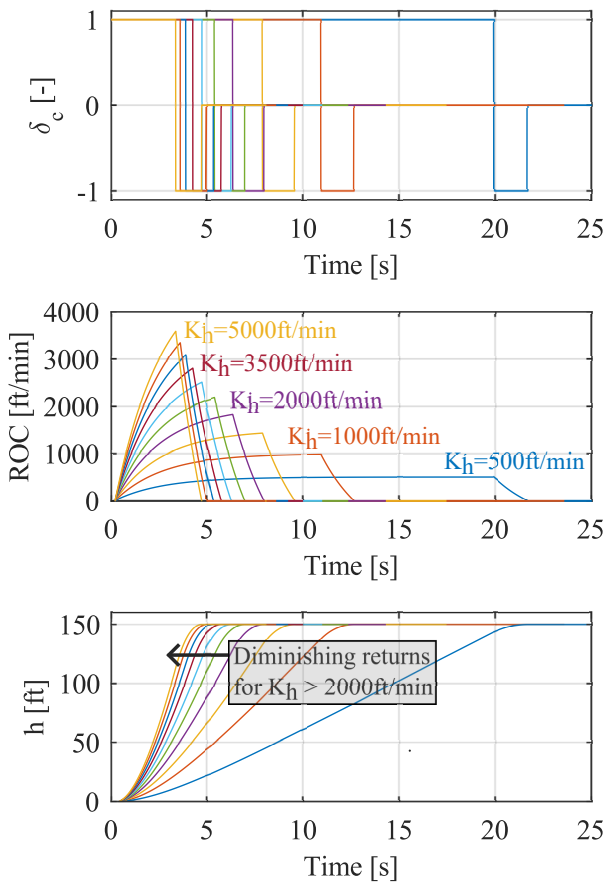

Figure 11. Example of MRM collective-climb simulations for $V = 60\,\text{kn}$ (for Big Air collective MTE sizing)

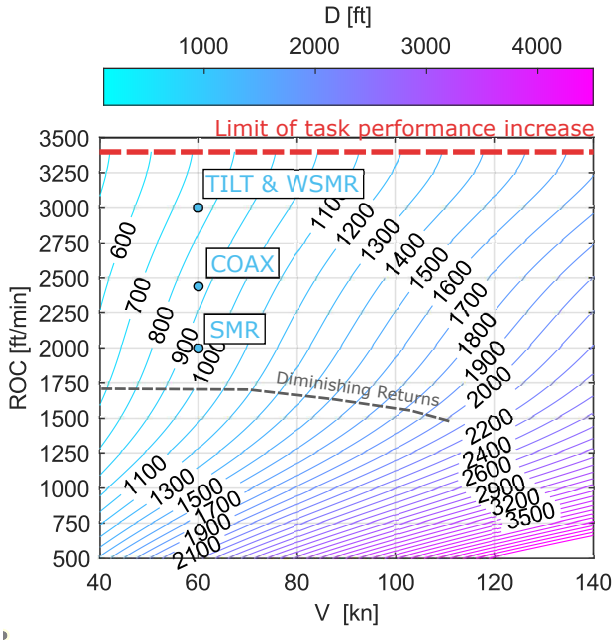

Figure 12. Big Air collective climb MTE sizing chart: D values vs. ROC and velocity V

Piloted simulation runs were conducted using DLR's AVES Simulator to ascertain viable time delay adjustment in calculating course size. In this setup, the pilot was instructed to execute a timed Big Air MTE climb task under varying course sizes. The flight model was tuned to have a time constant in the heave axis of $T_{\dot{h}} = 2.5\,\text{s}$ to lie exactly on the level 1/2 HQR boundary selected for MRM task sizing. The critical transition point, where the pilot needed to significantly alter the control strategy to meet the task's time requirement, was identified at a delay of $\Delta T = 3.0\,\text{s}$. Beyond this threshold, there was a notable increase in pilot workload, consequently diminishing the time efficiency in maneuver completion. Remarkably, a similar delay value of 3.5 s has also been corroborated in the study by Xin et al. (Ref. 3), specifically in the context of the Break Turn MTE. This was later on evaluated and verified by Berger and Ott (Ref. 11) in flight test trials using a UH-60M platform. For this reason, the ideal time to complete and the course sizing value D resulting from Eq. 14 for collective climb MTEs was modified by the addition of $T_{\text{react},\delta_x} = 3.0\,\text{s}$.

In analyzing pitch climb reaction time demands, drastically lower values were needed. It was found that, in general, an additional reaction time of only 0.3 s was adequate for achieving task demands that are in line with pilot expectations. Reaction time is composed of two key components: stimulus time, the duration for sensory information to reach the brain, and response time, the interval needed for the brain to process this information and initiate a muscle reaction. The average human reaction time is approximately 284 milliseconds, as discussed by Kranzler (Ref. 22), which aligns with the identified requirement for effective pitch climb maneuvers. Thus, the desired time to complete the Big Air MTE T_{des} is given by:

$$T_{\text{des},\delta_c} = T_{\text{ideal},\delta_c} + T_{\text{react},\delta_c} \quad \text{with} \quad T_{\text{react},\delta_c} = 3.0\,\text{s} \tag{15}$$

$$T_{\text{des},\delta_x} = T_{\text{ideal},\delta_x} + T_{\text{react},\delta_x} \quad \text{with} \quad T_{\text{react},\delta_x} = 0.3\,\text{s} \tag{16}$$

$$D_{\delta_i} = V T_{\text{des},\delta_i} \tag{17}$$

A preliminary analysis of the pilot's control strategy was performed to understand the difference of a factor of 10 between adequate reaction time terms based on the primary control input method.

For the pilot's control compensation, Padfield et al. (Ref. 23) suggested the control attack metric A_η, which measures the size and rapidity of a pilot's control inputs. The control attack characterizes each discrete control input. It is defined as the ratio of the peak rate of control displacement, $\dot{\eta}$, to the magnitude of the change in the inceptor displacement, $\Delta\eta$:

$$A_\eta = \frac{\dot{\eta}}{\Delta\eta} \tag{18}$$

Examination of the peak rate of control deflections reveals a distinct variance in pilot attack behaviors across the two primary control methods, as shown in Fig. 13. Specifically, when required to predominantly manage the flight path using pitch inputs, pilots exhibited a peak deflection rate approximately

twice as high ($\dot{\eta}_{\delta_x} \approx 50\,\%\,\mathrm{s}^{-1}$) as that observed with collective inputs ($\dot{\eta}_{\delta_c} \leq 25\,\%\,\mathrm{s}^{-1}$). In other words, during pitch inputs, the pilots showed more aggression and thus matched the assumed step-input control strategy better, thus lowering the needed reaction time modification.

Several hypotheses emerge to explain the reduced aggressiveness in collective inceptor usage. One plausible reason is the avoidance of adverse cross-coupling effects, which are typically more pronounced in this axis than in pitch. Additionally, ingrained training practices that emphasize over-torque prevention – irrespective of the presence of torque protection systems – may inhibit pilots from increasing the level of attack on the collective. Another consideration is the pilot's perception of approaching performance limits. For collective inputs, the critical constraint is often the available torque, typically monitored through visual checks of the torque gauge. This method, however, may be subject to lag due to delayed gauge response. In contrast, when flying in pitch, the limiting factor is usually the normal load factor. As most rotorcraft lack G-meters, pilots rely on sensory feedback and training to recognize signs of excessive stress, such as alterations in handling characteristics or unusual noises.

Though these considerations may contribute to the difference in reaction time allocation, the precise rationale underlying these observed differences in pilot behavior remains inadequately understood and warrants further investigation.

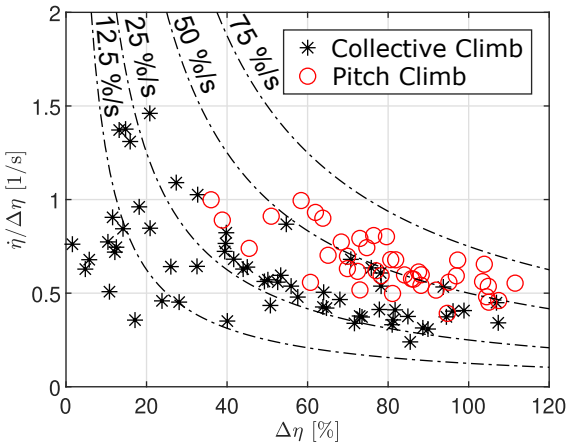

Figure 13. Variation in $\dot{\eta}$ during the Super Combined MTE. The data encompasses 10 trial runs with a Coaxial-Pusher (with torque protection) and Single-Main-Rotor model (without torque protection), executed by two pilots, a range of response types (Table 2), forward velocities of 60 kn **and** $0.8V_h$

Cyclic Roll - Flight Path Response Model

The MTE sizing requirements for the Giant Slalom (lateral flight path changes) were adopted from the computations introduced for the Break Turn MTE by Xin et al. (Ref. 24). The Break Turn MTE is a non-precision, aggressive maneuver composed of a 90° heading change designed for evasive combat maneuvering. In the Break Turn MTE, the pilot must perform an aggressive flight path change within the aircraft's operational flight envelope (OFE).

The Break Turn MTE has an ideal time to complete T_{ideal}, which is based on the aircraft maximum attainable bank angle ϕ_{lim}, the airspeed at which the task is flown V, and the aircraft agility as defined by its time to bank requirement from MIL-STD-1797 (Ref. 16). The time to bank requirement in MIL-STD-1797 (Ref. 16) is based on aircraft Class and Flight Phase Category. Since this task is an aggressive maneuver, it falls under Flight Phase Category A: "nonterminal Flight Phases that require rapid maneuvering..." Details on the calculation of T_{ideal} are provided Xin et al. (Ref. 24) and are expanded on in Berger and Ott (Ref. 11).

Roll Rate Response Similar to the Break Turn MTE, the lateral flight path changes here are assumed to occur at the maximum required roll acceleration $\dot{p}_{\max}$ which is calculated from the time to bank requirement in MIL-STD-1797 (Ref. 16) as:

$$\dot{p}_{\max} = \frac{2\phi_{\text{req}}}{t_{\text{req}}^2} \tag{19}$$

where t_{req} is the time to achieve the specific bank angle ϕ_{req} from MIL-STD-1797 (Ref. 16).

The time to bank requirements and associated maximum roll acceleration are listed in Table 1 for the different Aircraft Categories, as defined in MIL-STD-1797 (Ref. 16).

As shown in Fig. 2, the Giant Slalom MTE is based on an $L = 100$ ft lateral deviation. The course sizing D is based on the airspeed, the maximum roll acceleration $\dot{p}_{\max}$, and finally a target bank angle ϕ_{target}, which sets the maximum required bank angle to complete the maneuver. Based on review of existing Slalom MTE flight data, as well as high-speed slalom simulation data and pilot feedback, the recommended target bank angle for this maneuver is $\phi_{\text{target}} = 30$ deg.

Figure 14 shows an example course sizing calculation for the Giant Slalom MTE at $V = 160$ kn for a Class IV aircraft. Given the maximum roll acceleration and target bank angle ϕ_{target}, the maneuver is flown banking right, then left, then right again in a continuous manner with the constraints of reaching (and not exceeding) the target bank angle ϕ_{target} during the maneuver and returning to the starting heading and original ground track line at the end of the maneuver. This results in the target bank angle ϕ_{target} being achieved in the middle section of the maneuver at the maximum lateral offset from the centerline, as shown in Fig. 14.

The blue lines in Fig. 14 show the maneuver with no neutral time (i.e., roll rate is always varying and bank angle is never held constant during the maneuver). This results in a maximum lateral offset of around 13 ft as shown in Fig. 14(b). In order to achieve the desired lateral offset of $L = 100$ ft, a neutral time is added where the bank angle is held at each extreme. The red lines in Fig. 14 show the maneuver with neutral time added to achieve a lateral offset of $L = 100$ ft. Figure 14(b) shows the resulting course sizing $D \approx 1400$ ft.

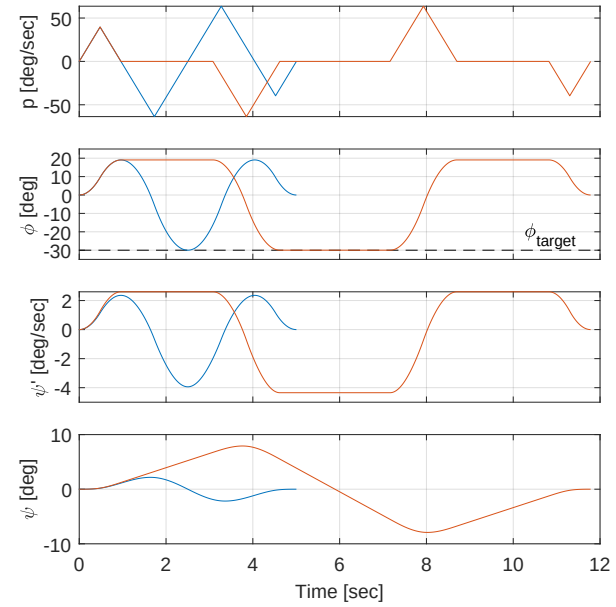

(a)

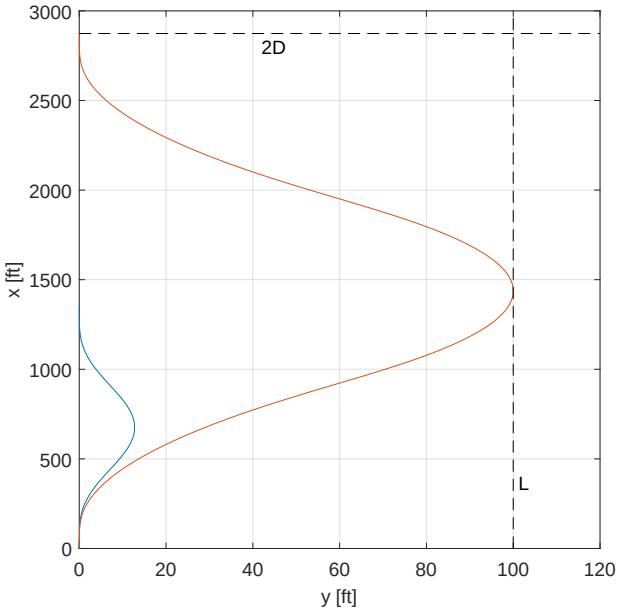

(b)

Figure 14. Example of MRM cyclic-roll simulation for $V = 160$ kn showing (a) time history and (b) course sizing.

Based on this sizing approach, the Giant Slalom MTE course size D is given in Fig. 15 as a function of airspeed V and target bank angle ϕ_{target}.

SIMULATION SETUP

Aircraft Models

Four aircraft models were used in the study: a scout/attack-class Single Main Rotor (SMR), a scout/attack-class Winged-

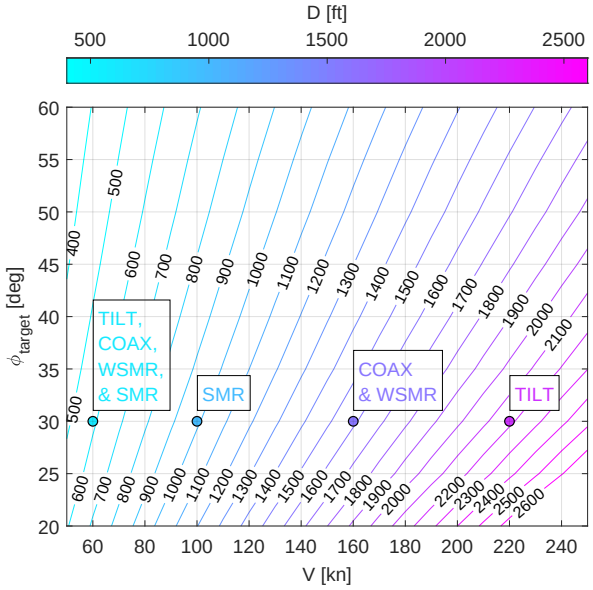

Figure 15. Giant Slalom MTE sizing chart: D values vs target bank angle ϕ_{target} and airspeed V.

Single-Main-Rotor (WSMR), a scout/attack-class lift offset coaxial helicopter with compound thrust pusher propeller (COAX), and a utility-class tiltrotor (TILT). The configurations were chosen to cover the full range of conventional (enduring fleet representative) to advanced (Future Vertical Lift representative) rotorcraft.

The flight dynamics of the single main rotor helicopter (SMR) were developed to be representative of DLR's ACT/FHS research platform helicopter (Fig. 16). The flight dynamics of the SMR helicopter were calculated using the HeliWorX real-time model. The details of the flight model are documented by Hamers and Gruenhagen (Ref. 25).

The WSMR, COAX, and TILT models were developed using HeliUM-A, U.S. Army Combat Capabilities Development Command Aviation & Missile Center's (DEVCOM AvMC) in-house flight-dynamics modeling software tool developed as an extension to the University of Maryland's HeliUM simulation model, described in detail by Juhasz et al. (Ref. 26) and Celi (Ref. 27). HeliUM-A uses a finite-element approach to model flexible rotor blades with coupled non-linear flap/lag/torsion dynamics to capture structural, inertial, and aerodynamic loads along each blade segment. Blade, wing, and fuselage aerodynamics come from non-linear lookup tables, and the rotor air wakes are modeled using a dynamic inflow model.

Table 1. Time to Bank Requirements and Maximum Roll Acceleration

Class	Req. Bank Angle ϕ_{req} [deg]	Req. Time t_{req} [s]	Roll Acceleration $\dot{p}_{\text{max}}$ [deg/s^2]
I	60	1.3	71.0
II	45	1.4	45.9
III	30	2.0	15.0
IV	50	1.1	82.6

The WSMR, COAX, and TILT models are generic and are not meant to represent specific industry designs. The WSMR configuration, shown in Fig. 17, was derived and scaled from the UH-60A (overall geometries, main rotor, and tail rotor properties), as well as the XV-15 and Bo-105 HGH (wing and empennage properties). The configuration has a gross weight of 15 000 lbs and maximum continuous power speed of $V_{MCP} = 200$ kn. A detailed description of the development of the WSMR flight dynamics model is provided by Lopez et al. (Ref. 28).

The COAX configuration, shown in Fig. 18, was scaled down from a generic utility-class coaxial-pusher configuration. The scaling method used and details of the design are provided by Padthe et al. (Ref. 29). The configuration has a gross weight of 15 000 lbs and maximum continuous power speed of $V_{MCP} = 210$ kn.

The TILT configuration, shown in Fig. 19, was derived from scaling geometric, inertial, and structural properties of the XV-15, V-22, and the notional NASA Large Civil Tilt-Rotor 2 (LCTR2). The configuration has a gross weight of 32 000 lbs and maximum continuous power speed of $V_{MCP} = 280$ kn. A detailed description of the development of the TILT flight dynamics model is provided by Berger et al. (Ref. 30).

Figure 16. DLR's ACT/FHS research helicopter

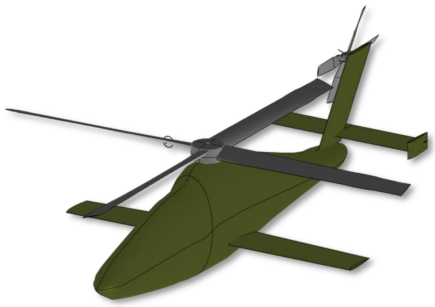

Figure 17. Generic winged single main rotor (WSMR) schematic

Control Laws All models were evaluated for different flight control response types and hold modes, ranging from basic Stability Augmentation Systems (SAS) to Rate Command hold (RC), Attitude Command (AC), and up to Flight Path Rate Command (FPRC) and including variations of Height Holds (HH) and Velocity Holds (VH). An overview of all tested response types and hold modes is given in Table 2. For the COAX and WSMR, the control laws change the response type depending on the airspeed. Here, the configurations for the two velocities that were evaluated during the simulator trials are listed, representing backside and frontside of the power required curve maneuvering: 60 kn and 80% of the maximum speed in level flight with maximum continuous power V_h. More information about the control laws of the WSMR, COAX, and TILT is provided in Berger et al. (Ref. 31) and Berger et al. (Ref. 32).

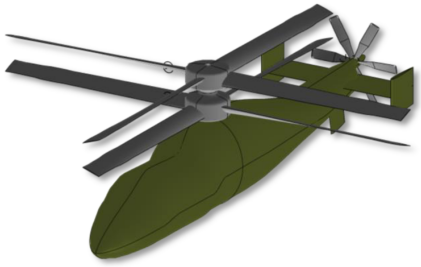

Figure 18. Generic coaxial-pusher (COAX) schematic

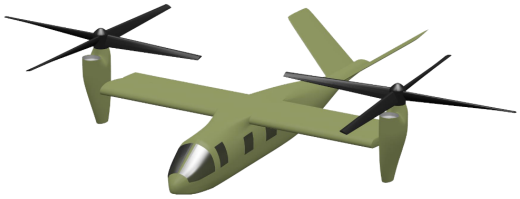

Figure 19. Generic tiltrotor (TILT) schematic

Specific MTE Sizing For MTE evaluation, the course sizes were determined by analyzing select evaluation points for each of the four aircraft configurations under two distinct velocity conditions: 60 kn, indicative of operations on the backside of the power curve, and $0.8V_h$, representing frontside power curve operations.

For the COAX and WSMR configurations, assessments were

Config.	V	Lon.	Lat.	Pedal	Col.	Thumb
SMR						
A	60 kn-100 kn	SAS	SAS	SAS	Direct	-
B	60 kn-100 kn	AC-AH	AC-AH	SAS	Direct	-
C	60 kn-100 kn	AC-VH	AC-AH	RC-DH	RC-HH	-
COAX						
C_0	60 kn-160 kn	RC-AH	RC-AH	SC-TC	Direct	PC-RC
C_1	60 kn	RC-AH	RC-AH	RC-TC	RC-HH	PCRC
C_1	160 kn	RC-AH	RC-AH	SC-TC	Direct	PCRC
C_4	60 kn	AC-VH	AC-AH	RC-TC	RC-HH	LAC+VH
C_4	160 kn	AC-AH	AC-AH	SC-TC	Direct	LAC+VH
WSMR						
C_0	60 kn-160 kn	RCAH	RCAH	SC+TC	Direct	-
C_1	60 kn-160 kn	RCAH	RCAH	SC+TC	RC-HH	-
C_4	60 kn-160 kn	AC-VH	AC-AH	RC+HH	Direct	VHS
TILT						
C_1	60 kn	RC-AH	RC-AH	RC+TC	Direct	NTRC
C_1	220 kn	GC-AoAH	RC-AH	SC+TC	Direct	NTRC
C_4	60 kn	FPRC-FPH	RC-AH	RC+TC	LAC-VH	-
C_4	220 kn	FPRC-FPH	RC-AH	SC+TC	LAC-VH	LAC+VH

Table 2. FCS configurations for the four rotorcraft models used in the study

Figure 20. AVES - Air Vehicle Simulator at DLR Braunschweig

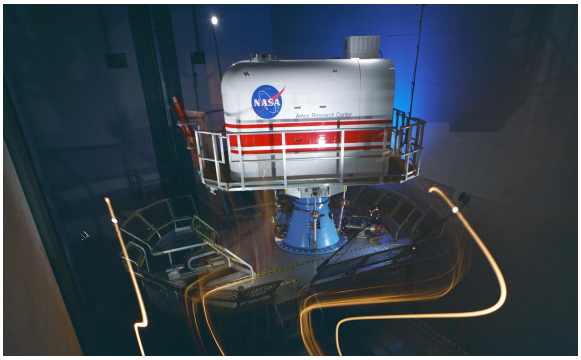

Figure 21. VMS - Vertical Motion Simulator at Ames Research Center

conducted at $0.8V_h = 160\,\text{kn}$, with a ROC of $2000\,\text{ft}\,\text{min}^{-1}$ and a maximum normal load factor of $n_z = 2$ for pitch climbs, as illustrated in Fig. 8. At 60 kn, a collective climb control strategy was assumed, with the ROC set at $2500\,\text{ft}\,\text{min}^{-1}$ for the coaxial-pusher and $3000\,\text{ft}\,\text{min}^{-1}$ for the winged-single main rotor, as depicted in Fig. 12. Giant Slalom sizing for the COAX and WSMR is shown in Fig. 15.

The TILT configuration underwent evaluation at $0.8V_h = 220\,\text{kn}$ and an ROC of $2000\,\text{ft}\,\text{min}^{-1}$ at $n_z = 2$ for pitch climbs, detailed in Fig. 10. For collective climbs at 60 kn, the evaluation considered an ROC of $3000\,\text{ft}\,\text{min}^{-1}$, as shown in Fig. 12. Giant Slalom sizing for the TILT is shown in Fig. 15.

Lastly, the SMR was analyzed at $0.8V_h = 100\,\text{kn}$ and an ROC of $1600\,\text{ft}\,\text{min}^{-1}$ at $n_z = 1.8$ for pitch climbs, with findings presented in Fig. 9. For collective climbs at 60 kn, the single main rotor's performance was evaluated with a ROC of $2000\,\text{ft}\,\text{min}^{-1}$, as outlined in Fig. 12. Giant Slalom sizing for the SMR is shown in Fig. 15.

Facilities

DLR Air Vehicle Simulator The simulation facility AVES is shown in Fig. 20. The simulator features four interchangeable modules: an Airbus A320, a Dassault Falcon 2000LX, a Eurocopter EC135, as well as a single aisle passenger cabin. These modules can be exchanged via a Roll-on / Roll-off system to utilize a full-sized six-degree of freedom, hexapod motion platform, or a fixed-base platform. The EC135 cockpit on the motion-base platform was used for the investigations described in this paper. The projection system consists of 9 LED projectors, each with a resolution of 1920x1200, which provide a horizontal Field of View (FOV) of 240° and a vertical FOV of $-55°$ to 40° as described by Duda et al. (Ref. 33). The inceptor configuration consisted of a center stick, standard pedals, and a collective using pull-for-power logic. A heads-down primary flight display and First Limit Indicator (FLI) were provided.

NASA Vertical Motion Simulator The Vertical Motion Simulator (VMS) is shown in Fig. 21. The VMS provides 6-degree of freedom motion with 60 ft of vertical and 40 ft of lateral travel. The side-by-side rotorcraft cockpit, known as T-cab, was used, which provides a 180-degree field of view to the pilot (right seat) as well as a chin window. The inceptor configuration consisted of a side stick attached to the right-hand side of the pilot seat, standard pedals, and a collective using pull-for-power logic. A heads-up display, depicted on the external world view, kept the pilot focused outside flying rather than on the instrumentation.

RESULTS

MTE Evaluation

The study aimed to thoroughly assess the proposed MTEs to evaluate their effectiveness in evaluating HQs and simulating real-world military operational scenarios. To achieve this objective, a pilot questionnaire was utilized, originally designed and used by Klyde et al. (Ref. 12). The questionnaire was administered to a cohort of eight experienced pilots, evenly distributed between the German and US Armies. Each pilot participated in piloted motion simulations, contributing diverse perspectives and extensive flight experience to the research. The questionnaire results presented in Fig. 22 were obtained after piloted simulation runs of the proposed MTEs were conducted both at AVES using the SMR model and at VMS using the COAX, WSMR and TILT models. Two German army and two US army pilots (4/8) had the opportunity to fly all the configurations at both simulator facilities before giving their final answers. Additionally, two German test pilots participated exclusively in the AVES simulations, and two US army pilots exclusively in the VMS studies before evaluating the MTEs. Fig. 22 combines all final questionnaire answers of the participating pilots according to the three MTEs.

Analysis of the questionnaire responses revealed a notable level of agreement among the pilots regarding various aspects of the MTEs. Specifically, the pilots acknowledged that the MTEs adequately represent operational task elements, suggesting a degree of fidelity to real-world military aviation operations. The pilots also generally agreed on the clarity and precision of the MTE definitions.

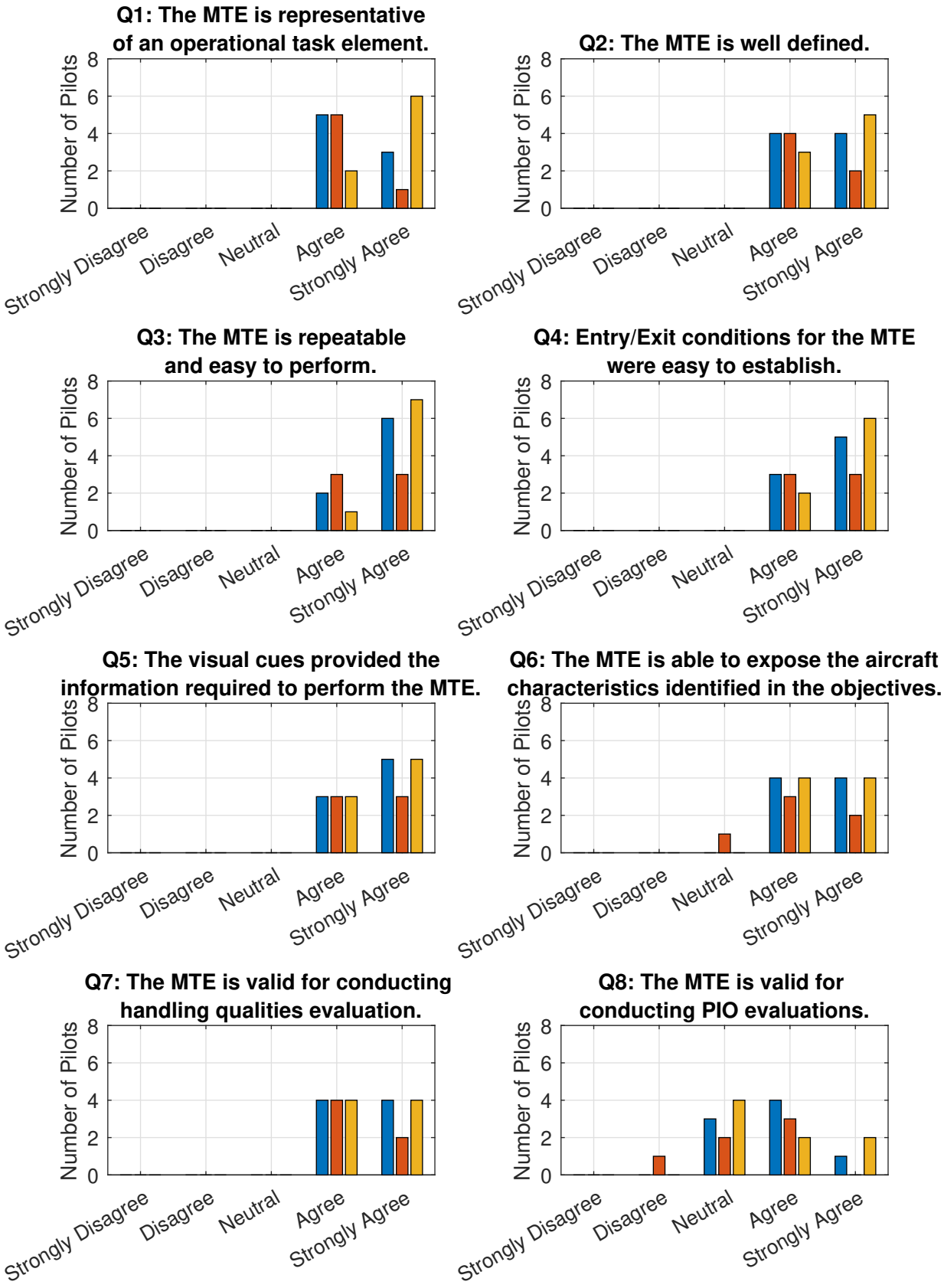

Figure 22. Results from MTE Questionnaire for MTE Big Air, Giant Slalom and Super Combined

This aspect is essential for ensuring consistent testing conditions across different pilots, facilitating reliable assessments of handling qualities and aircraft characteristics. Additionally, the pilots agreed on the MTEs' repeatability and ease of performance, which suggests that the tasks could serve as standardized measures.

Similarly, pilots found establishing entry and exit conditions for the MTEs straightforward, indicating potential ease of integration into routine training and evaluation protocols. Pilots generally agreed on their adequacy regarding visual cues provided in the simulations. This suggests that the MTEs effectively utilize environmental and instrumental references necessary for executing tasks in simulated flight conditions. Furthermore, pilots concurred that the MTEs could effectively reveal aircraft characteristics as defined in the study objectives, allowing for detailed analysis of aircraft performance under various operational conditions.

In conclusion, the collective pilot feedback synthesized from the questionnaire supports the potential utility of the MTEs for assessing handling qualities aspects for the low-level flight profile.

Ratings & Task Performance

After confirming the validity of the MTEs, piloted simulations were performed for HQ evaluation using the before-introduced flight models representing the following rotorcraft categories: the Scout/Attack-Class Coaxial Pusher (COAX), Scout/Attack-Class Winged-Single-Main-Rotor (WSMR), Utility-Class Tiltrotor (TILT), and Scout/Attack-Class Single Main Rotor (SMR).

Each configuration was subjected to systematic testing and evaluation, focusing on the MTEs introduced in the "Proposed Tasks" section and further detailed in Appendices A-C. These evaluations were conducted under a variety of control laws (Tab. 2). These included Rate Command Attitude Hold (RCAH) and Attitude Command Attitude Hold (ACAH) for pitch and roll, Direct Stick to Head and Rate Command in heave, and advanced modes like Height Hold (HH) and Velocity Hold (VH). Additionally, performance at two distinct speeds was analyzed: forward flight at 60 knots, representative of backside of the power curve maneuvering, and high-speed forward flight, corresponding to 80% of the maximum continuous power velocity, representing maneuvering on the frontside of the power curve.

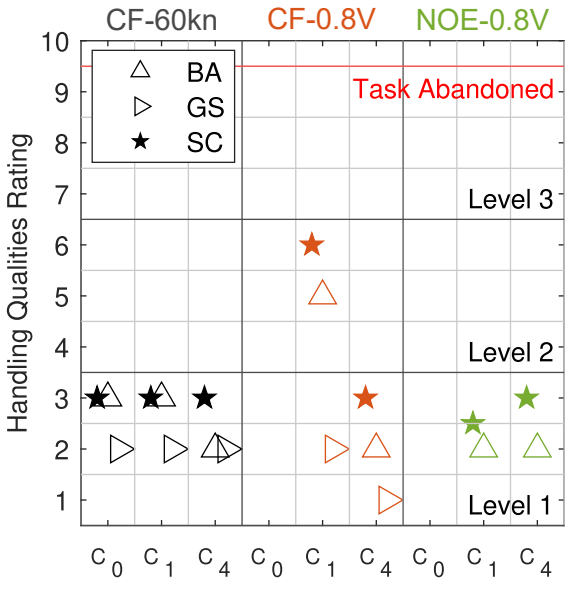

Figure 23. Handling Qualities Ratings for COAX

Figure 23 shows the HQR results for the COAX. Regarding performance on the backside of the power curve, the coaxial-pusher configuration (Fig. 23, denoted as CF-60 kn) exhibited remarkably uniform ratings within a ± 1 Handling Qualities Rating (HQR) band, falling within Level 1. This uniformity suggests that pilots did not perceive significant differences in handling or identify specific deficiencies across the evaluated control laws. For the contour flight variation of the MTEs, that is variant (a.) as described in Appendix A-C Table 3-

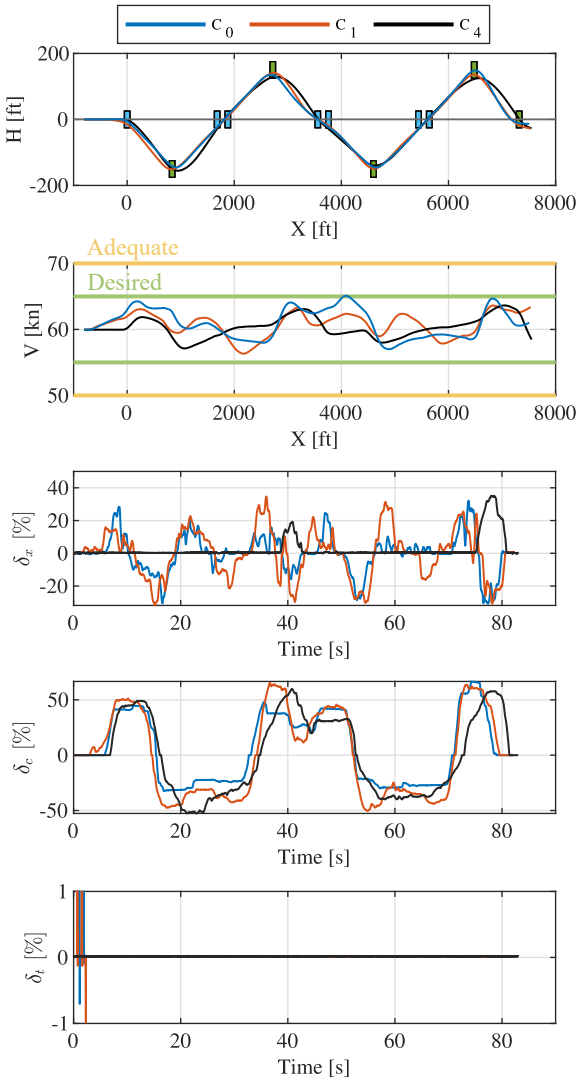

Figure 24. Task performance of COAX during Big Air MTE at $V = 60$ kn (BA-CF-60kn)

5, which requires to minimize airspeed excursions, the pilots adopted a classical control strategy. This involved primarily using the collective for flight path alterations and the pitch for velocity control instead of employing the pusher via a thumb button. Figure 24 presents the data on task performance and control inputs for the Big Air (BA) MTE under contour flight requirements. Notably, the introduction of velocity hold with Control Law 4 (C_4) enabled pilots to predominantly use collective inputs only, reducing HQRs from 3 to 2. Figure 25 presents sample results for the COAX Super Combined MTE flown at $0.8V_H = 160\,\text{kn}$.

In contrast to the previously mentioned configurations, the evaluations for the tilt-rotor (Fig. 26) and winged-single main-rotor (Fig. 27) configurations exhibited notable improvements with increasing levels of control system augmentation. Specifically, the ratings progressed from Level 2 to Level 1 when transitioning from C_1 to C_4 during the execution of the MTEs "Super Combined" (SC) and "Big Air" (BA). This enhancement in ratings was predominantly attributed to the implementation of the velocity hold mode. Pilot feedback highlighted that this feature significantly reduced the need for manual pitch inputs to regulate airspeed, simplifying the control process. In the context of operations on the frontside of the power curve, an analysis of the HQRs revealed that configurations employing additional airspeed control inceptors exhibited certain limitations.

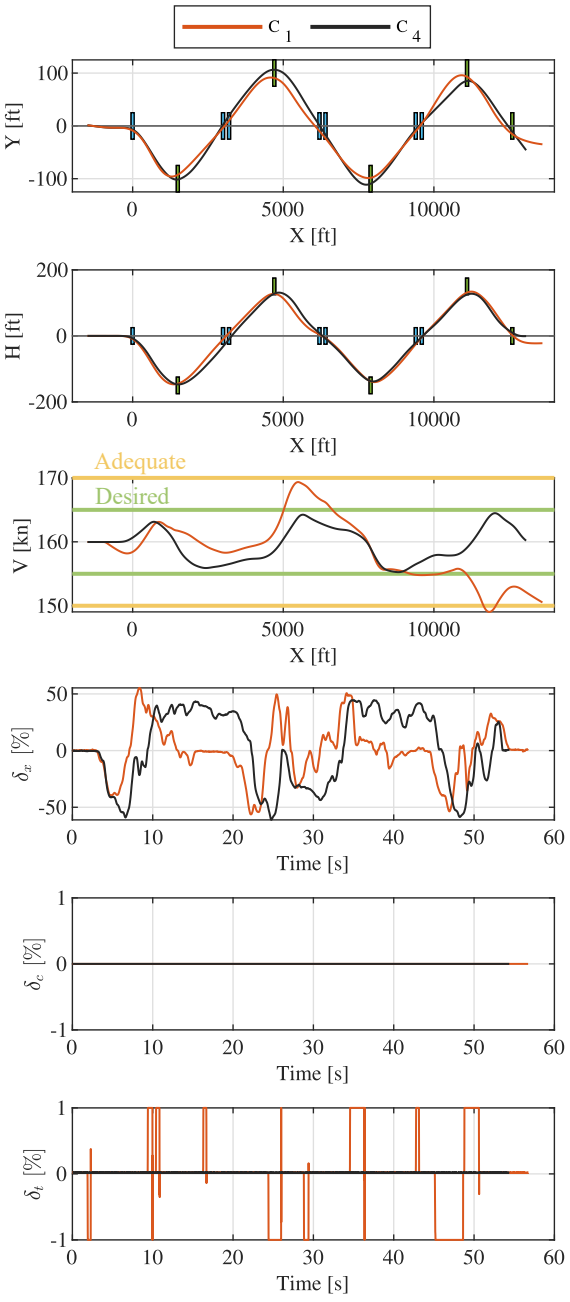

Figure 25. Task performance of COAX during Super Combined MTE at $0.8V_h = 160\,\text{kn}$ (SC-CF-0.8V)

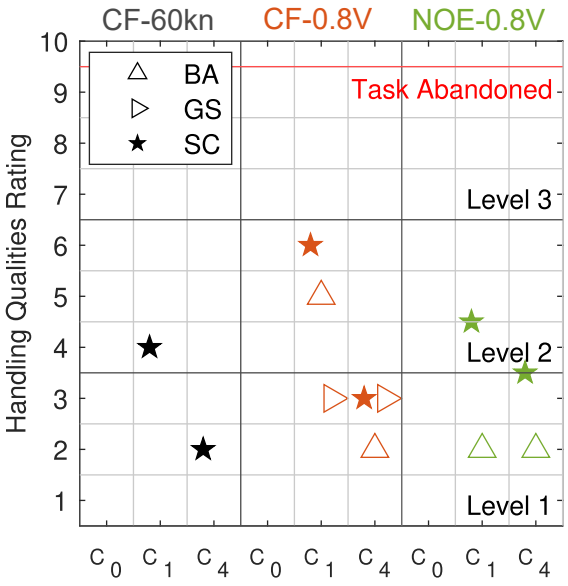

Figure 26. Handling Qualities Ratings for TILT

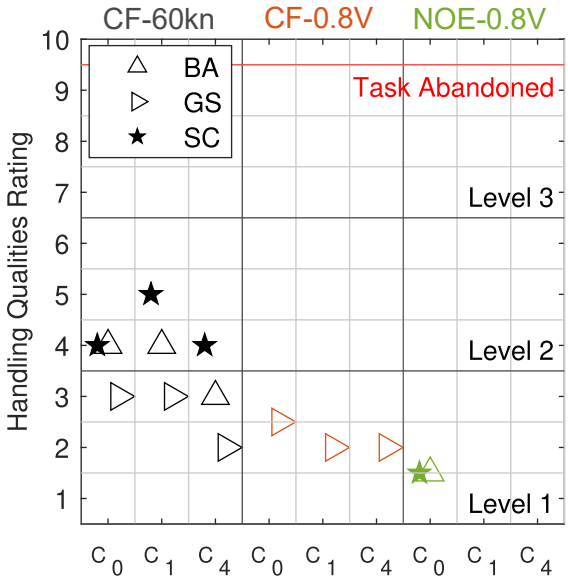

Figure 27. Handling Qualities Ratings for WSMR

Specifically, configurations such as the prop collective rate command for the coaxial pusher (illustrated in Fig. 23, under C_1), and the nacelle tilt rate command for the tilt-rotor (shown in Fig. 26, C_1) demonstrated deficiencies. These shortcomings were particularly pronounced for the contour flight variations of the proposed MTEs, allowing only small deviations in airspeed over the task duration - and in turn, requiring a high amount of precision in airspeed control.

Pilots reported experiencing a "sluggish" response in the correlation between the input from the inceptor (thumb wheel) and the consequent alterations in the aircraft's speed. This delay in response time detrimentally impacted the handling qualities, posing challenges in achieving precise control. A velocity hold mode was integrated as part of Control Law 4 in response to this issue.

This modification significantly improved the HQRs, elevating them to the Level 1 range, as evidenced in Fig. 25. This advancement indicates that the fundamental models inherently possess the capacity to meet the desired performance standards. Nevertheless, it becomes apparent that the primary challenge to realizing optimal performance resides in the effective integration and refinement of the inceptor system. Intriguingly, this specific issue was not observed during the standard testing procedures of MTEs and was not identified in the extensive evaluations using established quantitative handling qualities criteria.

The Single Main Rotor (SMR) configuration received HQRs at the cusp of Level 1 and Level 2 (as shown in Fig. 28), particularly for the backside contour flight MTE variants (Fig. 29). Pilot feedback indicated that this was primarily due to collective coupling motions. Compensation for these motions required pilots to lead with forward and left cyclic inputs and right pedal inputs. A control strategy involving slow and smooth collective input was adopted to ensure precise lead inputs. This approach necessitated a compromise on the attack aggressiveness to maintain flight predictability and minimize coupled attitude excursions, a phenomenon elaborated in Fig. 13.

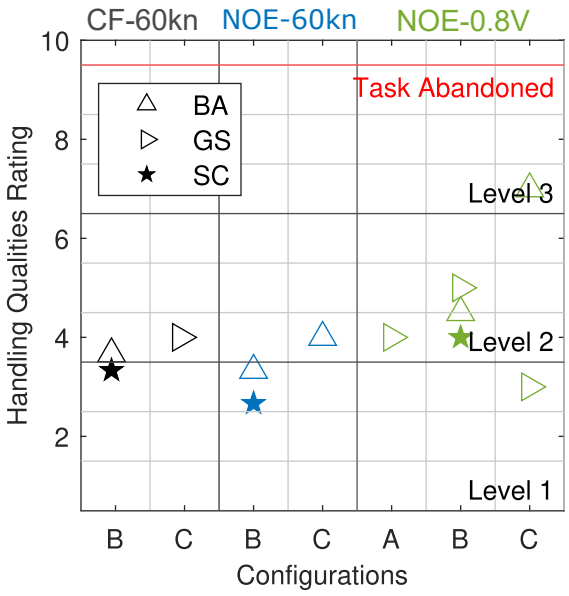

Figure 28. Handling Qualities Ratings for SMR

Furthermore, a notable decline in HQRs was observed when transitioning from Level 1 with C_B to Level 2 with C_C, for the backside NOE MTE variants. Control Law C incorporated a height hold mode in the heave axis, which provided inadequate control authority according to pilot evaluations. This insufficiency hindered the pilots' ability to achieve the desired levels of maneuvering aggressiveness.

The issue becomes more complex when examining scenarios on the frontside of the power curve. With C_B, the pilots adopted an intuitive control strategy, utilizing moderate cyclic pitch inputs to attain the required ROC for successful task completion.

However, Control Law C (C_C) presents a challenge, as it features a coupling of the RC-HH in heave to the collective position. Consequently, this design causes the controller to actively maintain altitude when pulling the cyclic stick aft ac-

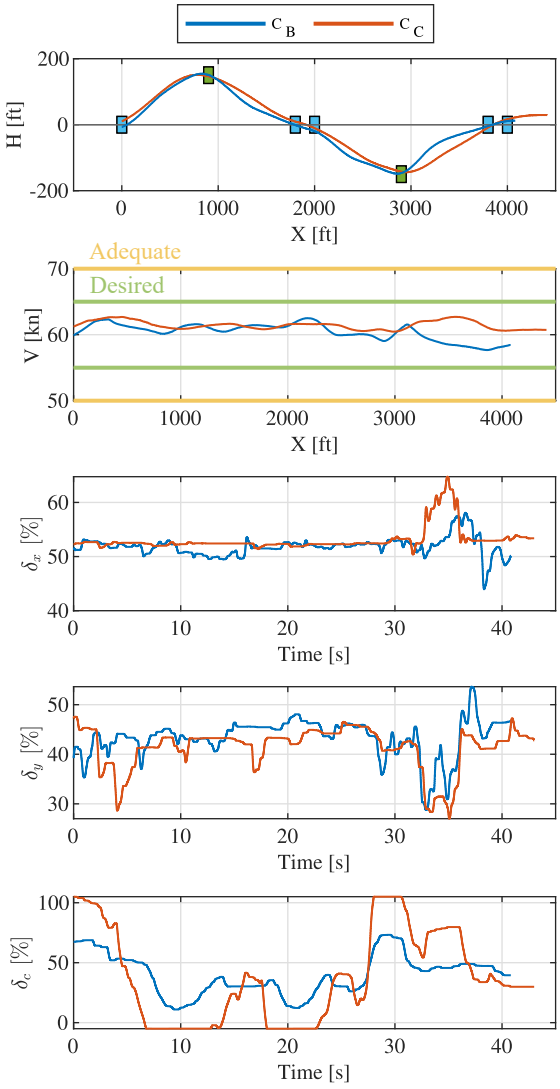

Figure 29. Task performance of SMR during Big Air MTE at $V = 60\,\text{kn}$ (BA-CF-60kn)

tively, inadvertently suppressing the intended ROC build-up. To counteract this, pilots had to rely on additional collective inputs (Fig. 30), which did not produce the necessary ROC rate to navigate climbs successfully and dives through the gates.

This flight control characteristic directly contravenes the Pitch Control Power Requirement for Level 1 as stipulated in MIL-DTL-32742 (Ref. 4), which mandates that: "For Level 1, from trimmed, unaccelerated flight, the rotorcraft shall achieve the load factor limits specified in the Operational Flight Envelopes during turns or pull-up/push-over maneuvers."

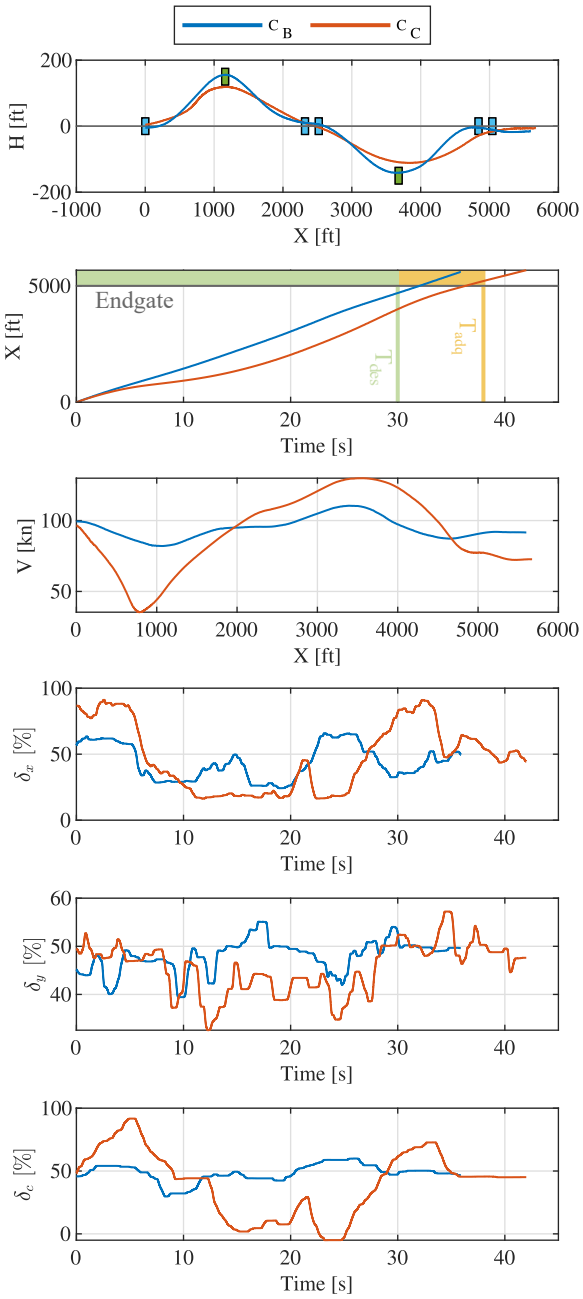

Figure 30. Task performance of SMR during Big Air MTE at $0.8V_H = 100\,\text{kn}$ (BA-NOE-0.8V)

However, the criteria for Level 2 state the following two requirements:

(a) Adequate pitch control authority to accelerate from 45 knots to the maximum level flight airspeed and decelerate back to 45 knots at a constant altitude.

(b) Sufficient pitch authority to maintain altitude with full power at 45 knots and minimum power at maximum level flight airspeed.

In this context, the SMR in C_C configuration complies with Level 2 requirements (a) and (b), but the restrictions on ROC due to the height hold implementation prevent it from achieving Level 2 HQRs. Particularly, the requirement (b) addresses situations where pitch authority is maintained with varying collective input but does not account for scenarios requiring pitch control with constant collective and an expected vertical flight path change, as in the Level 1 requirement.

A simplistic solution would suggest that meeting the Level 1 Pitch Control Power Requirement is sufficient for achieving at least Level 2 in the proposed MTEs. However, this approach may be misleading and, in the authors' view, does not adhere to the clear intent that standards should strive for.

Thus, it is proposed that the requirement be modified to include the specific case of height hold modes for high agility low-level tasks as an additional vertical flight path control power requirement. Though this is out of the scope of this paper and sound guidance for future work, the following key points are proposed for the potential requirement changes:

1. This requirement should explicitly address the rotorcraft's capability to effectively adjust its Rate of Climb (ROC) and Rate of Descent (ROD) while in (out of) height hold modes.

2. It should specify a minimum ROC and ROD that must be achievable if the height hold mode does not disengage automatically without compromising the control authority or stability of the aircraft.

In contrast to the aforementioned scenarios, a marked improvement in the HQRs was observed for lateral flight path change MTEs. Specifically, the ratings advanced from Level 2 under C_B to Level 1 with the implementation of C_C, as demonstrated in Fig. 31. This enhancement can be attributed to the introduction of velocity hold and height hold modes, which significantly reduced the need for pilot compensation. As a result, the task was effectively simplified to involve lateral cyclic inputs primarily.

CONCLUSIONS

This paper describes the development and evaluation of three Mission Task Elements designed for flight path handling qualities assessment for low-level operations. The task dimensions were designed to be scalable according to OFE performance limits. Eight Pilots rated the MTEs "Big Air", "Giant

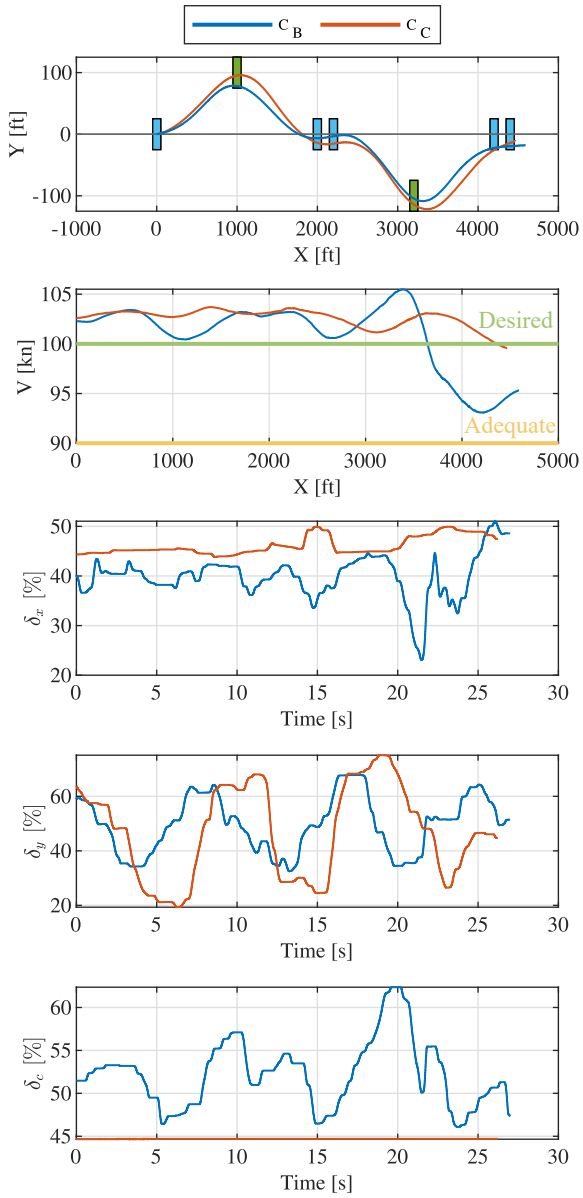

Figure 31. Task performance of SMR during Giant Slalom MTE at $0.8V_H = 100$ kn (GS-CF-0.8V)

Slalom", and "Super Combined" as to whether they represent operational task elements, expose the aircraft characteristics identified in the objectives, and are valid for conducting handling qualities evaluations. These ratings were obtained via piloted simulation using four distinct rotorcraft configurations under various control laws and airspeed.

The following conclusions are drawn:

1.) Novel Mission Task Elements tailored for low-level mission flight profiles are introduced, which received high acceptance from pilot participants, underlining their operational relevance and effectiveness. The MRM method produced MTE sizing guidelines that were in accordance with pilots' expectations regarding varying aircraft configurations and airspeed. The MTEs identified handling quality deficiencies that are particularly critical for missions at low altitudes, thereby demonstrating their utility in enhancing flight safety and applicability to design guidance.

2.) The results showed that configurations allowing additional control over airspeed significantly improved Handling Qualities Ratings (HQRs) in the low-speed regime compared to traditional configurations and were generally favored by pilots. This improvement was less pronounced during high-speed maneuvering, where the characteristics of additional control inputs, like thumb wheels, became crucial for maintaining precise speed control during contour flight. Introducing a Velocity Hold (VH) feature was particularly effective in addressing these challenges, as it mitigated performance sluggishness and simplified the control task from three-axis to two-axis, substantially easing the pilot's workload during complex maneuvers.

3.) Conclusion 2 highlights the need for effective integration and refinement of inceptor systems to optimize aircraft control. Consequently, these findings emphasize the necessity for predictive criteria tailored to flight speed control inceptors, such as thumb wheels acting on pusher propellers or nacelle angle adjustment.

4.) The study highlighted a challenge with specific variants of height hold control laws, wherein coupling the RC-HH in heave to collective position suppresses the intended ROC build-up. This contravenes the Level-1 Pitch Control Power Requirement outlined in MIL-DTL-32742 (Ref. 4). While complying with Level-2 requirements, the restrictions on ROC due to height hold prevent achieving Level-2 HQRs. This reveals a gap in the guidelines, suggesting a need for modification to include specific requirements for height hold modes in low-level tasks. Proposed changes address the ability to make ROC and Rate of Descent (ROD) adjustments out-of or in height hold mode without compromising aircraft control authority or stability.

ACKNOWLEDGMENTS

This research was undertaken within the US-German Project Agreement – Advanced Technologies for Rotorcraft (PA-ATR). The German part was funded by the German Federal Ministry of Defence. The authors would like to thank the Federal Office of Bundeswehr Equipment, Information Technology and In-Service Support (BAAINBw) for their support, as well as the Bundeswehr Technical Center for Aircraft and Aeronautical Equipment (WTD61) and the participating pilots for their invaluable support of this activity. Furthermore, the authors extend their gratitude to the committed support teams of the NASA VMS and DLR's AVES simulator facilities, without whose assistance this work would not have been possible.

REFERENCES

*

1. LTC Rafael Ichaso. Russian Air Force's Performance in Ukraine - Air Operations: The Fall of a Myth. *The Journal of the Joint Air Power Competence Centre (JAPCC)*, Journal Edition 35, February 2023.

2. Roy L. Brewer, Frank Conway, and Ray Mulato. Further Development and Evaluation of a New High-Speed Acceleration / Deceleration ADS-33 Mission Task Element. In *American Helicopter Society's International 74th Annual Forum & Technology Display Proceedings*, Pheonix, Arizona, May 2018.

3. Hong Xin, William C Fell, Joseph Horn, Cody E. Fegely, Paul D. Ruckel, James M. Rigsby, Roy L. Brewer, Frank P. Conway, Ray. Mulato, David H. Klyde, Sean P. Pitoniak, LTC Carl R. Ott, and Christopher L. Blanken. Further Development and Piloted Simulation Evaluation of the Break Turn ADS-33 Mission Task Element. *Journal of the American Helicopter Society*, 67 (4):pp. 1–14(14), October 2022. ISSN 2161-6027. doi: 10.4050/JAHS.67.042003.

4. MIL-DTL-32742. Handling Qualities for Military Rotorcraft. Detail Specification, U.S. Department of Defense, March 2023.

5. ADS-33E-PRF. Performance Specification Handling Qualities Requirements for Military Rotorcraft. Aeronautical Design Standard, U.S. Army Aviation and Missile Command (AvMC), March 2000.

6. Tom Berger, Mark B. Tischler, and Joseph F. Horn. High-Speed Rotorcraft Pitch Axis Response Type Investigation. In *Proceedings of the Vertical Flight Society 77th Annual Forum*, Virtual, Online, May 2021. Vertical Flight Society. ISBN 978-1-71383-001-6. doi: 10.4050/F-0077-2021-16793.

7. Heinz-Jürgen Pausder and Dieter Hummes. Flight Tests for the Assessment of Task Performance and Control Activity. In *AHS/NASA Specialists' Meeting on Helicopter Handling Qualities*, Moffett Field, California, April 1982. American Helicopter Society (AHS).

8. Kenneth H. Landis and Edwin W. Aiken. An Assessment of Various Side-Stick Controller/Stability and Control Augmentation Systems for Night Nap-of-Earth Fl ight Using Piloted Simulation. In *AHS/NASA Specialists' Meeting on Helicopter Handling Qualities*. American Helicopter Society (AHS), 1982.

9. Courtland C. Bivens. Directional Handling Qualities Requirements for Nap of the Earth (NOE) Tasks. In *41st Annual Forum of the Amrican Helicopter Society*, Fort Worth, Texas, May 1985.

10. James C. Bumbaugh, John K. Tritschler, Christopher Mattei, Michael M. Mosher, and Robert Barthelmes. Flight Test Evaluation of Proposed High-Speed Break Turn Mission Task Element. In *Vertical Flight Society (VFS) 75th Annual Forum*, Philadelphia, Pennsylvania, May 2019. doi: 10.4050/F-0075-2019-14594.

11. Tom Berger and LTC Carl R. Ott. Flight Test Assessment of the Break Turn and High-Speed Acceleration/Deceleration Mission Task Elements using a UH-60M Black Hawk. In *Vertical Flight Society's 75th Annual Forum & Technology Display*, Philadelphia, Pennsylvania, May 2019. doi: 10.4050/F-0075-2019-14599.

12. David H. Klyde, Sean P. Pitoniak, P. Chase Schulze, Paul Ruckel, James Rigsby, Hong Xin, Cody E. Fegely, William C. Fell, Roy Brewer, Frank Conway, Ray Mulato, Joe Horn, LTC Carl R. Ott, and Chris L. Blanken. Piloted Simulation Evaluation of Attitude Capture and Hold MTEs for the Assessment of High-Speed Handling Qualities. In *Vertical Flight Society's 74th Annual Forum & Technology Display Proceedings*, Pheonix, Arizona, May 2018.

13. David H. Klyde, Sean P. Pitoniak, P. Chase Schulze, Paul Ruckel, James Rigsby, Cody E. Fegely, Hong Xin, William C. Fell, Roy Brewer, Frank Conway, Ray Mulato, Joe Horn, LTC Carl R. Ott, and Chris L. Blanken. Piloted Simulation Evaluation of Tracking MTEs for the Assessment of High-Speed Handling Qualities. In *Vertical Flight Society's 74th Annual Forum & Technology Display Proceedings*, Pheonix, Arizona, May 2018.

14. David L. Key, Chris L. Blanken, Roger H. Hoh, David G. Mitchell, and Bimal L. Aponso. Background Information and User's Guide for Handling Qualities Requirements for Military Rotorcraft. Special Report SR-RDMR-AD-16-01, U.S. Army Aviation and Missile Research, Development and Engineering Center (AMRDEC), 2015.

15. Tom Berger. *Handling Qualities Requirements and Control Design for High-Speed Rotorcraft*. Dissertation in Aerospace Engineering, The Pennsylvania State University, December 2019.

16. MIL-STD-1797. Flying Qualities of Piloted Aircraft. Interface Standard, U.S. Department of Defense, 2004.

17. Douglas Thomson and Kevin Ferguson. Manoeuvrability assessment of a hybrid compound helicopter configuration. In *40th European Rotorcraft Forum*, volume 2, pages 748–760, Southhampton, U.K., September 2014.

18. MathWorks. Find minimum of unconstrained multivariable function using derivative-free method, February 2024. URL `https://de.mathworks.com/help/matlab/ref/fminsearch.html`.

19. Padfield G. D. Helicopter handling qualities and control: is the helicopter community prepared for change?

In *Proceedings Royal Aeronautical Society Conference: Helicopter Handling Qualities and Control*, 1988.

20. Carl J. Ockier. Flight Evaluation of the New Handling Qualities Criteria Using the BO 105. In *49th American Helicopter Society Annual Forum*, St. Louis, USA,, May 1993. American Helicopter Society (AHS).

21. Gareth D. Padfield. *Helicopter Flight Dynamics*. Blackwell Science Ltd, Oxford, new edition edition, January 2000. ISBN 978-0-632-05607-1.

22. John H. Kranzler. Mental Chronometry. In Norbert M. Seel, editor, *Encyclopedia of the Sciences of Learning*, pages 2180–2182. Springer US, Boston, MA, 2012. ISBN 978-1-4419-1428-6. doi: 10.1007/978-1-4419-1428-6_238.

23. Gareth Padfield, M.T. Charlton, J.P. Jones, and R. Bradley. Where Does The Workload Go When Pilots Attack Manoeuvres? An Analysis of Results from Flying Qualities Theory and Experiment. In *20th European Rotorcraft Forum*, Amsterdam, The Netherlands, September 1994. Deutsche Gesellschaft Fuer Luft Und Raumfahrt (DGLR).

24. Hong Xin, Cody E Fegely, William C Fell, Joseph F Horn, Paul D Ruckel, James M Rigsby, Roy L Brewer, and Frank P Conway. Further Development and Piloted Simulation Evaluation of the Break Turn ADS-33 Mission Task Element. In *AHS International 74th Annual Forum & Technology Display*, Pheonix, Arizona, May 2018.

25. M. Hamers and W. von Gruenhagen. Nonlinear Helicopter Model Validation Applied to Realtime Simulations. In *Proc. of the AHS 53rd Annual Forum, Virginia Beach, VA, USA, April 29 - May 1, 1997*, pages 958–972, 1997.

26. Ondrej Juhasz, Roberto Celi, Tom Berger, Mark B. Tischler, and Christina M. Ivler. Flight Dynamic Simulation Modeling of Large Flexible Tiltrotor Aircraft. In *American Helicopter Society's 68nd Annual Forum*, Fort Worth, Texas, May 2012. American Helicopter Society (AHS) International.

27. Roberto Celi. Analytical Simulation of ADS-33 Mission Task Elements. In *American Helicopter Society's 63rd Annual Forum*, Virginia Beach, VA, May 2007. American Helicopter Society (AHS).

28. Mark J. S. Lopez, Tom Berger, Eric L. Tobias, Emily D. Glover, and Ashwani K. Padthe. Seeking Lift Share: Design Tradeoffs for a Winged Single Main Rotor Helicopter. In *Vertical Flight Society Annual Forum & Technology Display - Forum 78*, Fort Worth, Texas, May 2022. The Vertical Flight Society. doi: 10.4050/F-0078-2022-17547.

29. Ashwani K. Padthe, Emily D. Glover, Mark J. S. Lopez, Tom Berger, Eric L. Tobias, and Ondrej Juhasz. Design, Modeling, and Flight Dynamics Analysis of Generic Lift-Offset Coaxial Rotor Configurations. In *Vertical Flight Society Annual Forum & Technology Display - Forum 78*, Fort Worth, Texas, May 2022. The Vertical Flight Society. doi: 10.4050/F-0078-2022-17580.

30. Tom Berger, Ondrej Juhasz, Mark J. S. Lopez, Mark B. Tischler, and Joseph F. Horn. Modeling and control of lift offset coaxial and tiltrotor rotorcraft. *CEAS Aeronautical Journal*, 11(1):191–215, January 2020. ISSN 1869-5590. doi: 10.1007/s13272-019-00414-0.

31. Tom Berger, Chris L. Blanken, Jeff A. Lusardi, Mark B. Tischler, and Joseph F. Horn. Coaxial-Compound Helicopter Flight Control Design and High-Speed Handling Qualities Assessment. *Journal of the American Helicopter Society*, 67(3):pp. 98–113(16), July 2022. ISSN 2161-6027. doi: 10.4050/JAHS.67.032008.

32. Tom Berger, Chris L. Blanken, Jeff A. Lusardi, Mark B. Tischler, and Joseph F. Horn. Tiltrotor Flight Control Design and High-Speed Handling Qualities Assessment. *Journal of the American Helicopter Society*, 67(3):pp. 114–128(15), July 2022. ISSN 2161-6027. doi: 10.4050/JAHS.67.032009.

33. Holger Duda, Sunjoo K. Advani, and Mario Potter. Design of the DLR AVES Research Flight Simulator. In *AIAA Modeling and Simulation Technologies (MST) Conference*, Boston, MA, August 2013. American Institute of Aeronautics and Astronautics. doi: 10.2514/6.2013-4737.

34. George E. Cooper and Robert P. Harper. The use of pilot rating in the evaluation of aircraft handling qualities. Technical Report NASA TN D-5153, National Aeronautics and Space Administration, Washington, D.C., April 1969.

APPENDIX A: BIG AIR

a. Objectives. The maneuver is designed to reproduce rapid changes in altitude during low-to-earth contour & NOE obstacle avoidance flight. The objectives are:

- Evaluate ability to make aggressive vertical flight path changes.
- Identify potentially excessive flight path lags.
- Check for undesirable handling qualities during aggressive vertical flight path changes.
- Evaluate speed control during aggressive maneuvering (Contour Flight version).
- Check for handling qualities degradation and undesirable coupling between pitch, roll, heave, and yaw during aggressive maneuvering.
- Check for overly complex power management.

b. Description of the maneuver. Initiate the maneuver in level unaccelerated flight at Velocity V_t and lined up with the center line of the test course. Perform a series of climbs and dives at 'D'-ft intervals. The reversals shall be separated at least H=150ft vertically from the centerline. Between the reversals, the middle sections should have a separation of at least C=200ft. Complete the maneuver on the centerline in coordinated straight flight.

c. Description of the test course. The courses for this task are laid out with a series of gates. Fig. 32 shows the suggested course layout.

d. Task performance requirements determination. For a mission-relevant aircraft configuration at velocity V , determine the two gate distance values (a.) D_{CF} based on the primary control strategy for vertical flight path changes at constant airspeed (Contour Flight) and the gate value distance of (b.) D_{NOE} based on the primary control strategy for maximum agility vertical flight path changes (NOE) based on the following rules:

1. Primary control strategy – Raise collective: Determine the maximum achievable Rate of Climb (ROC) during constant airspeed collective climb. From Fig.12 determine the corresponding reference D-value.
2. Primary control strategy - Pitch angle change: Determine the maximum achievable Rate of Climb (ROC) during constant airspeed pitch climb. Determine the corresponding maximum achievable Load Factor (n_z) during constant airspeed pitch climb. From Fig. 7-10 determine the corresponding reference D-value.

f. Performance standards. Calculate T_{des} using the obtained D_{NOE}-value using Eq. 20. Note that Fig. 32 shows only one half of the course, with the second being either a repetition or mirror image of the first half.

$$T_{\text{des}} = \frac{8D_{NOE} + 5C}{V} \tag{20}$$

The evaluations should be performed using both task requirements variants (a.) and (b.), which are given in the table below.

	GVE	Course Size	Abbreviation
DESIRED PERFORMANCE			
Maintain altitude & position within ±X feet during gate fly through	25		
MCP excursion shall not exceed	Operational Limits		
(a.) Maintain Airspeed of at least ±X knots during the maneuver	5	D_{CF}	BA-CF
(b.) Complete the maneuver within X seconds	T_{des}	D_{NOE}	BA-NOE
ADEQUATE PERFORMANCE			
Maintain altitude & position within ±X feet during gate fly through	25		
MCP excursion shall not exceed	Operational Limits		
(a.) Maintain Airspeed of at least ±X knots during the maneuver	10	D_{CF}	BA-CF
(b.) Complete the maneuver within X seconds	$T_{\text{des}} + 8$	D_{NOE}	BA-NOE

Table 3. Big Air MTE Performance Standards

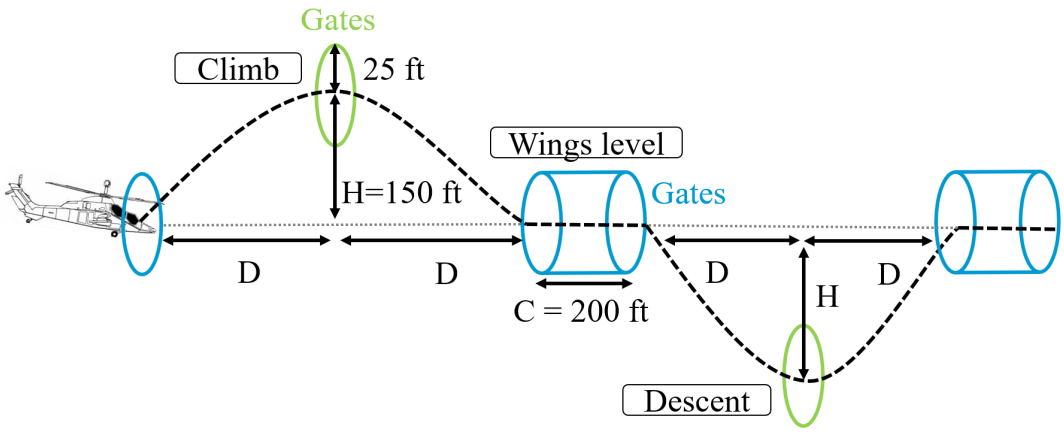

Figure 32. Suggested Big Air MTE course cueing

APPENDIX B: GIANT SLALOM

a. Objectives. The maneuver is designed to ensure that handling qualities do not degrade during aggressive lateral flight path changes under roll axis inputs. The objectives are:

- Evaluate ability to make aggressive lateral flight path changes.
- Identify potentially excessive flight path lags.
- Check for undesirable handling qualities during aggressive lateral flight path changes.
- Check for handling qualities degradation and undesirable coupling between pitch, roll, heave, and yaw during aggressive maneuvering.
- Check turn coordination for aggressive forward flight maneuvering.

b. Description of the maneuver. This MTE shall be performed for airspeeds on the backside and the frontside of the power required curve. Recommended values are 60 kn and $0.8V_H$. Start from an unaccelerated forward flight at and AGL $300-1000$ ft, fly through the course of gates. Maintain airspeed within task performance limits. Maintain altitude and position at the gates within task performance limits. The use of auxiliary propulsion control to regulate airspeed is acceptable

c. Description of the test course. The courses for this task are laid out with a series of gates. Fig. 33 shows the suggested course layout.

d. Task performance requirements determination. Aircraft Classes in MIL-STD-1797 (Ref. 16) are used to particularize the requirements according to broad categories of intended use and are related qualitatively to maximum design gross weight and limit load factor. The following are the definitions for Classes I–IV as defined in MIL-STD-1797 (Ref. 16):

- **Class I**: Small, light air vehicles (e.g., light utility, primary trainer, or light observation)
- **Class II**: Medium weight, low-to-medium maneuverability air vehicles (e.g., heavy utility, light or medium transport/cargo, tactical bomber, heavy attack)
- **Class III**: Large, heavy, low-to-medium maneuverability air vehicles (e.g., heavy transport/cargo/tanker, heavy bomber)
- **Class IV**: High maneuverability air vehicles (e.g., fighter/interceptor, attack, tactical reconnaissance)

Flight Phase Categories are used to particularize the requirements according to the type of tasks that need to be accomplished. The following are the definitions for Flight Phase Categories A–C as defined in MIL-STD-1797 (Ref. 16):

- **Category A**: Nonterminal flight phases that require rapid maneuvering, precise tracking, or precise flight-path control (e.g., air-to-air combat, terrain following, close formation flying, precision hover)

- **Category B**: Nonterminal flight phases that are normally accomplished using gradual maneuvers and without precision tracking (e.g., climb, cruise, loiter)
- **Category C**: Terminal flight phases that are normally accomplished using gradual maneuvers and usually require accurate flight-path control (e.g., takeoff, power approach, landing)

Since the Break Turn MTE is an aggressive task, the time to bank requirements for Category A should be used, and are reproduced here in Table 1.

For a mission-relevant aircraft configuration at velocity V, determine the gate distance value D based on the target bank angle ϕ_{target} from Figure 15.

	GVE	Course Size
DESIRED PERFORMANCE Maintain altitude & position within ±X feet during gate fly through Maintain airspeed of at least X knots throughout the course Any oscillations or couplings shall not be	 25 0.8 V undesirable	 *D*
ADEQUATE PERFORMANCE Maintain altitude & position within ±X feet during gate fly through Maintain airspeed of at least X knots throughout the course Any oscillations or couplings shall not be	 50 0.7 V objectionable	 *D*

Table 4. Giant Slalom MTE Performance Standards

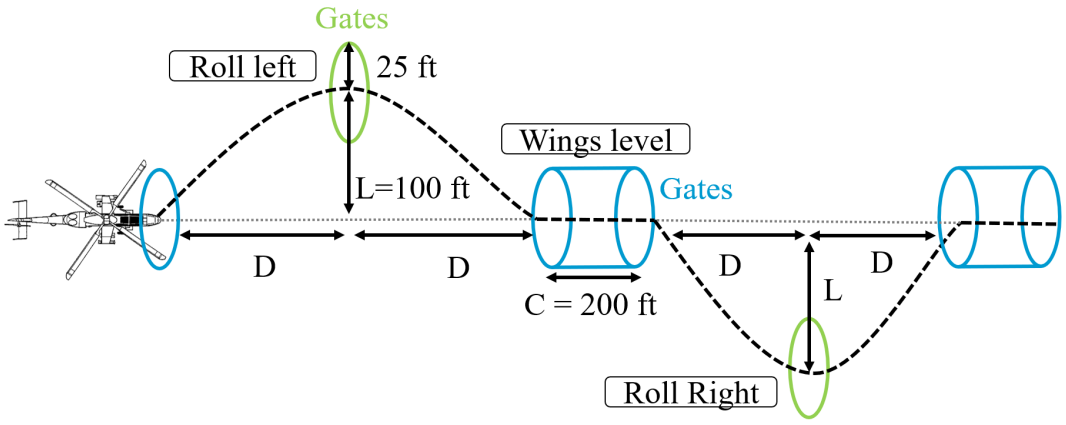

Figure 33. Suggested Giant Slalom MTE course cueing

APPENDIX C: SUPER COMBINED

a. Objectives. The maneuver is designed to reproduce rapid changes in altitude & lateral position during low-to-earth contour & NOE obstacle avoidance flight. The objectives are:

- Evaluate ability to make aggressive vertical and lateral flight path changes.
- Identify potentially excessive flight path lags.
- Check for undesirable handling qualities during aggressive vertical and lateral flight path changes.
- Evaluate speed control during aggressive maneuvering (Contour Flight version).
- Check for handling qualities degradation and undesirable coupling between pitch, roll, heave, and yaw during aggressive maneuvering.
- Check for overly complex power management.

b. Description of the maneuver. Initiate the maneuver in level unaccelerated flight at Velocity V_t and lined up with the center line of the test course. Perform a series of smooth turns at 'D'-ft intervals. The turns shall be separated at least $L = 100$ ft laterally and $H = 150$ ft vertically from the centerline. Between the turns, the middle sections should have a separation of at least C=200ft. Complete the maneuver on the centerline in a coordinated straight flight.

c. Description of the test course. The courses for this task are laid out with a series of gates. The suggested course layout is shown in Fig. 34

d. Task performance requirements determination. For a mission-relevant aircraft configuration at velocity V , determine the two gate distance values (a.) D_{CF} based on the primary control strategy for vertical flight path changes at constant airspeed (Contour Flight) and the gate value distance of (b.) D_{NOE} based on the primary control strategy for maximum agility vertical flight path changes (NOE) based on the following rules:

1. Primary control strategy – Raise collective: Determine the maximum achievable Rate of Climb (ROC) during collective climb and a bank angle of 30°. From Fig. 12 determine the corresponding reference D-value.
2. Primary control strategy - Pitch angle change: Determine the maximum achievable Rate of Climb (ROC) during constant airspeed pitch climb and a bank angle of 30 deg. Determine the maximum achievable Load Factor (n_z) during pitch climb and a bank angle of 30 deg. From Fig. 7-10 determine the corresponding reference D-value.

f. Performance standards. Calculate T_{des} using the obtained D_{NOE}-value using Eq. 21. Note that Fig. 34 shows only one half of the course, with the second being either a repetition or mirror image of the first half.

$$T_{\text{des}} = \frac{8D_{NOE} + 5C}{V_t} \tag{21}$$

The evaluations should be performed using both task requirements variants (a.) and (b.), which are given in the table below.

	GVE	Course Size	Abbreviation
DESIRED PERFORMANCE			
Maintain altitude & position within ±X feet during gate fly through	25		
MCP excursion shall not exceed	Operational Limits		
(a.) Maintain Airspeed of at least ±X knots during the maneuver	5	D_{CF}	SC-CF
(b.) Complete the maneuver within X seconds	T_{des}	D_{NOE}	SC-NOE
ADEQUATE PERFORMANCE			
Maintain altitude & position within ±X feet during gate fly through	25		
MCP excursion shall not exceed	Operational Limits		
(a.) Maintain Airspeed of at least ±X knots during the maneuver	10	D_{CF}	SC-CF
(b.) Complete the maneuver within X seconds	$T_{\text{des}} + 8$	D_{NOE}	SC-NOE

Table 5. Super Combined MTE Performance Standards

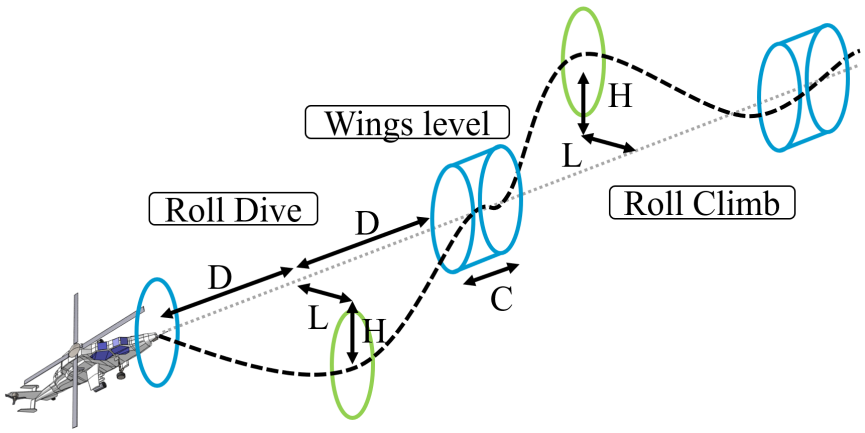

Figure 34. Suggested Super Combined MTE course cueing

APPENDIX D: RATING SCALES

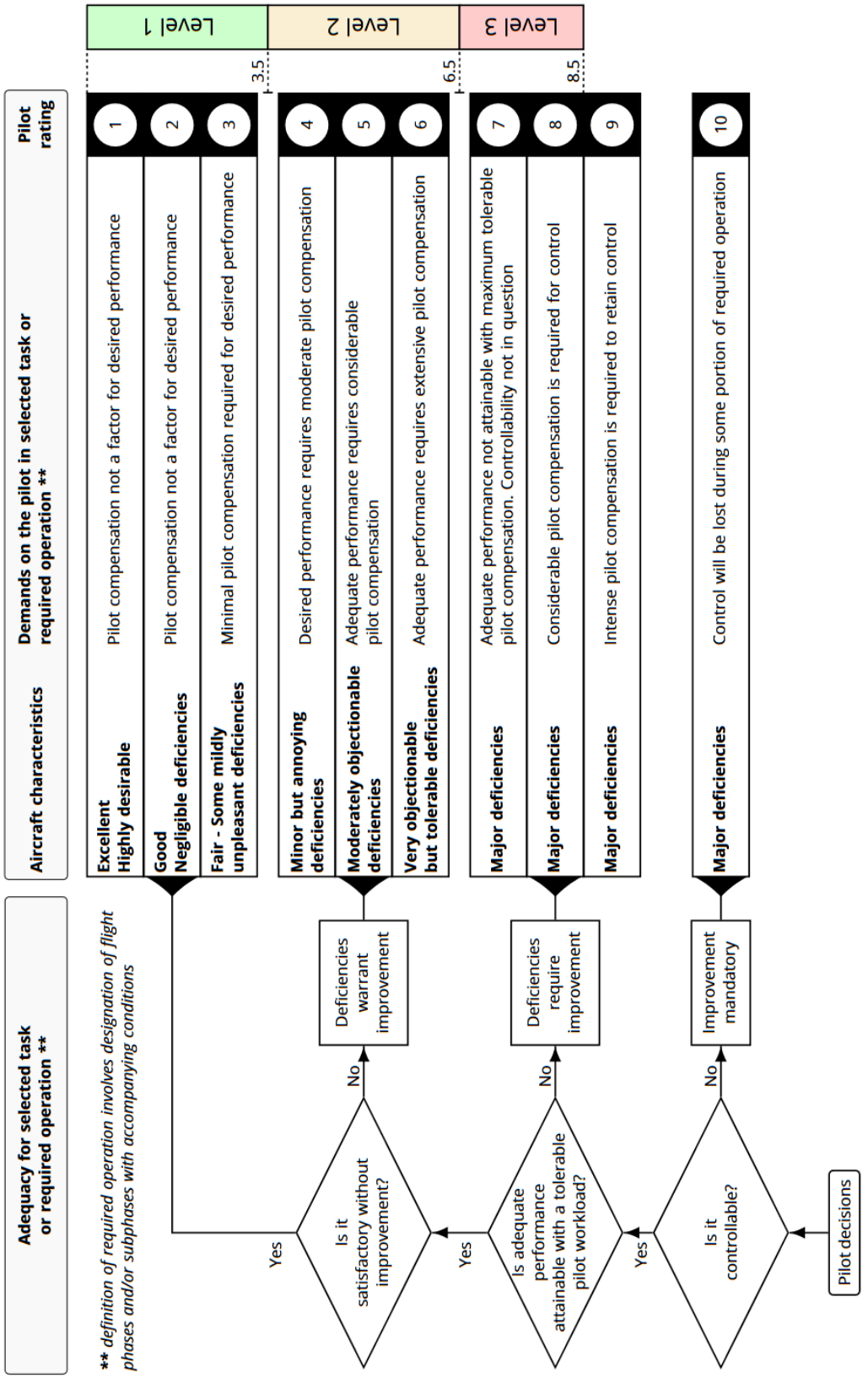

Figure 35. Cooper-Harper Handling Qualities Rating Scale (HQR) Cooper and Harper (Ref. 34) - level categorization according to MIL-DTL-32742 (Ref. 4)